

Development of targeted α therapy with Bi-213 and At-211 for the treatment of disseminated cancer

Synthesis and evaluation of pretargeting
components and radioimmunoconjugates

Anna Gustafsson-Lutz

Department of Radiation Physics
Institute of Clinical Sciences
Sahlgrenska Academy at the University of Gothenburg



UNIVERSITY OF GOTHENBURG
Gothenburg 2016

Cover illustration: To the left, a Bi-213-labeled polylysine-based effector molecule is depicted, and to the center right is a representation of a Bi-213-labeled antibody conjugated with CHX-A''-DTPA. The molecules are both intended to target tumor cells in vivo. In the background is a tissue section of a mouse peritoneum with a tumor visualized by α camera imaging. This cover illustration was prepared by Anna Gustafsson-Lutz and Tom Bäck.

Development of targeted α therapy with Bi-213 and At-211 for the treatment of disseminated cancer

© Anna Gustafsson-Lutz 2016
anna.gustafsson@radfys.gu.se

ISBN: 978-91-628-9720-8

E-publication: <http://hdl.handle.net/2077/41547>

Printed in Gothenburg, Sweden 2016

Ineko

*“Imagination was given to man to compensate for what he is not,
and a sense of humor was provided to console him for what he is”*

Oscar Wilde

Development of targeted α therapy with Bi-213 and At-211 for the treatment of disseminated cancer

Synthesis and evaluation of pretargeting components and radioimmunoconjugates

Anna Gustafsson-Lutz

Department of Radiation Physics, Institute of Clinical Sciences
Sahlgrenska Academy at the University of Gothenburg
Gothenburg, Sweden

ABSTRACT

Radioimmunotherapy (RIT) is a type of targeted cancer therapy. The concept behind RIT is to deliver cytotoxic ionizing radiation to tumor cells by attaching radionuclides to tumor-specific antibodies. The radioimmunoconjugates identify and bind to tumor cells, isolated or in clusters, wherever located and possibly indistinguishable using imaging procedures. Thus, RIT is aimed to be an adjuvant treatment such as chemotherapy, but in contrast to chemotherapy specifically targeted to tumor cells, sparing healthy cells and tissues.

RIT can however have unfavorable pharmacokinetics when administered systemically. To circumvent this problem, pretargeted RIT (PRIT) can be applied. In PRIT, administration of the therapeutic agents is divided into several steps. A modified antibody (pretargeting molecule) is first administered, and is allowed enough time (several hours) to localize the tumor cells. The unbound pretargeting molecules are then cleared from the circulation, either spontaneously or by the guidance of a clearing agent. As a final step, a radiolabeled molecule (effector) is administered, which has high affinity for the pretargeting molecule. The small size of the effector results in both rapid accumulation at the tumor site and fast blood clearance of unbound radioactivity. Thus, a higher tumor-to-normal tissue dose ratio is achievable with PRIT than RIT.

Different radionuclides can be used for different purposes in targeted therapy. In the treatment of micrometastases, alpha-emitting radionuclides are well-suited because of their short path length and high linear energy transfer. These properties result in high relative biological effectiveness (RBE) as well as a reduced dependence of oxygenation and

actively cycling cells when compared with nuclides emitting low-LET radiation. When properly targeted, alpha-emitters have high tumor-killing efficacy while sparing much of the normal healthy tissue due to their short range.

In this work, molecules for RIT utilizing the alpha-emitters ^{213}Bi and ^{211}At were produced and tested in vitro and in vivo. The principal evaluations of these molecules were focused on ovarian cancer therapy, utilizing a preclinical ovarian cancer mouse model. Results showed a therapeutic efficacy and a favorable biodistribution for the intraperitoneally injected alpha-RIT molecules. A new site-selective reagent for coupling ^{211}At to antibodies was also synthesized and evaluated. The resulting ^{211}At -labeled antibody conjugate showed good binding properties both in vitro and in vivo. Finally, agents for PRIT were synthesized, which exhibited promising properties for further preclinical evaluation in full PRIT systems.

Keywords: alpha particles, astatine, bismuth, MX35, ovarian cancer, polylysine, pretargeted radioimmunotherapy, radioimmunotherapy

ISBN: 978-91-628-9720-8

SAMMANFATTNING PÅ SVENSKA

Denna avhandling handlar om radioimmunoterapi (RIT), som är en intern strålterapi för behandling av cancer. Syftet med projektet var att skapa molekyler för RIT och för pretargeted radioimmunoterapi (PRIT) med de alfa-strålande radionukliderna ^{211}At och ^{213}Bi . Både RIT och PRIT är tilläggsbehandlingar för spridd cancer, och går ut på att cytotoxiska radionuklider levereras till tumörer med hjälp av tumörspecifika antikroppar. I RIT binds radionukliden direkt till den tumörspecifika antikroppen, varpå den injiceras. Eftersom antikroppar är mycket stora molekyler tar det vanligtvis många timmar för dem att lokalisera tumörerna vid systemisk behandling. I PRIT injiceras först en modifierad antikropp (pretargetingmolekyl) som tillåts cirkulera under lång tid för att lokalisera tumörerna. Därefter kan den radiomärkta molekylen, den s.k. effektorn, injiceras. Effektorn är en liten molekyl som har stor affinitet för pretargetingmolekylen. Den ansamlas därför snabbt vid tumörerna. De radiomärkta effektormolekylerna som inte bundit till tumörcellerna försvinner snabbt ifrån blodet p.g.a. den lilla storleken. Med PRIT kan man alltså en bättre farmakokinetik än med RIT, vilket leder till minskad bestrålning av normalvävnad, och därmed en ökad tumör-till-normalvävnadskvot av absorberad dos.

Vid behandling av mycket små tumörer, mikrometastaser, är alfa-strålande radionuklider fördelaktiga för målsökande terapier. De har en mycket kort räckvidd vilket gör att bestrålningen koncentreras på de små tumörerna, medan normalvävnad i stor utsträckning besparas. De har också en hög celldödande effekt inom sin korta räckvidd och är därför mycket effektiva vid tumörbehandling. Det finns endast ett fåtal alfa-strålare som passar och är tillgängliga för kliniskt bruk. Två av dem är ^{213}Bi och ^{211}At .

I detta projekt har molekyler för RIT med ^{213}Bi och ^{211}At producerats och utvärderats in vitro och in vivo i musförsök. Studierna var främst fokuserade på intraperitoneal terapi av äggstockscancer, och försök i tumörbärande möss visade minskad tumörförekomst hos de djur som behandlats. Behandlingarna demonstrerade också bra resultat i en toxicitetsutvärdering. Ett nytt reagens för att koppla ^{211}At till antikroppar har också syntetiserats och utvärderats. Det resulterande ^{211}At -märkta antikroppskonjugatet visade bra bindningsegenskaper in vitro och in vivo. Slutligen syntetiserades komponenter för PRIT, vilka visade lovande resultat för fortsatta studier i fullständiga PRIT-system.

LIST OF PAPERS

This thesis is based on the following studies, referred to in the text by their Roman numerals.

- I. Gustafsson AM, Bäck T, Elgqvist J, Jacobsson L, Hultborn R, Albertsson P, Morgenstern A, Bruchertseifer F, Jensen H, Lindegren S. *Comparison of therapeutic efficacy and biodistribution of ^{213}Bi - and ^{211}At -labeled monoclonal antibody MX35 in an ovarian cancer model.* Nuclear Medicine and Biology 2012; 1: 15-22.
- II. Gustafsson-Lutz A, Bäck T, Aneheim E, Albertsson P, Palm S, Morgenstern A, Bruchertseifer F, Lindegren S. *Therapeutic efficacy of α -radioimmunotherapy with different activity levels of ^{213}Bi -labeled monoclonal antibody MX35 in an ovarian cancer model.* Submitted
- III. Aneheim E, Gustafsson A, Albertsson P, Bäck T, Jensen H, Palm S, Svedhem S, Lindegren S. *Synthesis and evaluation of astatinated N-[2-(maleimido)ethyl]-3-(trimethylstannyl)benzamide immunoconjugates.* Accepted for publication in Bioconjugate Chemistry, 2016
- IV. Gustafsson-Lutz A, Bäck T, Aneheim E, Palm S, Morgenstern A, Bruchertseifer F, Albertsson P, Lindegren S. *Biotinylated and chelated poly-L-lysine as effector for pretargeting in cancer therapy and imaging.* Submitted
- V. Gustafsson-Lutz A, Bäck T, Aneheim E, Albertsson P, Press OW, Hamlin D, Lindegren S. *Galactosylated, biotinylated and charge-modified polylysine: evaluation as clearing agent for pretargeting in cancer therapy and imaging* Manuscript

All publications are reprinted by permission of the copyright holders.

CONTENT

ABBREVIATIONS.....	IV
1 INTRODUCTION	1
1.1 Metastatic cancer.....	1
1.2 Radioimmunotherapy	1
1.3 Pretargeted radioimmunotherapy.....	2
1.4 Antibodies and antibody-like molecules for RIT and PRIT.....	7
1.5 The target	8
1.6 Radionuclides for targeted therapy.....	9
1.7 Beta emitters.....	10
1.8 Alpha emitters	11
2 AIMS.....	13
3 BACKGROUND.....	15
3.1 Bismuth-213.....	15
3.2 The $^{225}\text{Ac}/^{213}\text{Bi}$ generator	15
3.3 Radiolabeling with ^{213}Bi	17
3.4 Astatine-211	17
3.5 Production and distillation of ^{211}At	18
3.6 Radiolabeling with ^{211}At	19
3.7 Ovarian cancer.....	20
3.8 Ovarian cancer tumor model.....	21
3.9 Antibodies for ovarian cancer targeting.....	21
4 METHODS	23
4.1 The chemistry of conventional radioimmunotherapy with ^{213}Bi and ^{211}At (Papers I-III).....	23
4.2 The chemistry of the synthesized pretargeting agents (Papers IV and V)	25
4.3 In vitro analyses.....	30
4.3.1 Molecular structure analysis	30
4.3.2 Radiochemical purity	30
4.3.3 Cell binding (Papers I-III)	31

4.3.4	Avidin binding (Paper IV)	31
4.4	Animal experiments	31
4.4.1	Therapeutic efficacy and toxicity of α -RIT in the ovarian cancer model (Papers I and II)	32
4.4.2	Biodistribution (Papers I, III-V)	32
5	RESULTS	35
5.1	In vitro results of the immunoconjugates for ^{213}Bi - and ^{211}At -labeling (Papers I-III)	35
5.1.1	Structure analysis	35
5.1.2	Radiochemical purity	35
5.1.3	Cell binding	35
5.2	In vivo results for the ^{213}Bi - and ^{211}At -labeled immunoconjugates (Papers I-III)	37
5.2.1	Therapeutic efficacy and toxicity	37
5.2.2	Biodistribution	39
5.3	In vitro and in vivo results of the polylysine-based effector for pretargeted radioimmunotherapy and -imaging (Paper IV)	44
5.3.1	Structure analysis	44
5.3.2	Radiochemical purity and avidin binding	44
5.3.3	Renal uptake study	44
5.4	In vivo results of the polylysine-based clearing agent for pretargeted radioimmunotherapy and -imaging (Paper V)	45
6	DISCUSSION	49
6.1	General	49
6.1.1	Papers I-II	50
6.1.2	Paper III	51
6.1.3	Papers IV-V	52
7	CONCLUSIONS AND FUTURE PERSPECTIVES	55
8	ACKNOWLEDGEMENTS	59
9	REFERENCES	61

ABBREVIATIONS

AES	Affinity enhancement system
ALA	5-Aminolevulinic acid
ATE	Activated tin ester
CA	Clearing agent
CD	Cluster of differentiation
DOTA	1,4,7,10-tetraazacyclododecane-1,4,7,10-tetraacetic acid
DSB	Double-strand break
DTPA	2-[Bis[2-[bis(carboxymethyl)amino]ethyl]amino]acetic acid
DTT	1,4-Dithiothreitol
EC	Electron capture
EDTA	2-((2-[Bis(carboxymethyl)amino]ethyl)(carboxymethyl)amino)acetic acid
FPLC	Fast protein liquid chromatography
HAMA	Human anti-mouse antibody
HER2	Human epidermal growth factor receptor 2
ICP-MS	Inductively coupled plasma mass spectrometry
IEDDA	Inverse electron-demand Diels-Alder reaction
ITLC	Instant thin layer chromatography
ITU	Institute for Transuranium Elements
K _d	Dissociation constant

LET	Linear energy transfer
mAb	Monoclonal antibody
MDS	Multiple damaged site
MORF	Morpholino oligomer
MSB	<i>N</i> -[2-(maleimido)ethyl]-3-(trimethylstannyl)benzamide
NAGB	Dendrimeric CA containing 16 biotinylated <i>N</i> -acetyl-galactosamine residues and a single biotin
NaPi2b	Sodium dependent phosphate transport protein 2b
OVCAR-3	Human epithelial ovarian carcinoma cell line 3
NIS	<i>N</i> -iodosuccinimide
PET	Positron emission tomography
PRII	Pretargeted radioimmunoimaging
PRIT	Pretargeted radioimmunotherapy
RCP	Radiochemical purity
RCY	Radiochemical yield
RIT	Radiomunotherapy
RT	Room temperature
SEM	Standard error of the mean
SPAAC	Strain-promoted azide-alkyne cycloadditions
SSB	Single-strand break
TCO	<i>trans</i> -Cyclooctene
TFF	Tumor-free fraction

1 INTRODUCTION

1.1 Metastatic cancer

In most fatal cancer diseases, the metastases rather than the primary tumor are the main cause of death [1]. Large single tumors can often be removed by surgery; however, metastases, depending on size and amount, can be very difficult to eradicate. Micrometastases are particularly difficult to treat since they cannot be detected by normal diagnosis methods, and are therefore an obstacle to enhancing survival rates [2]. Examples of cancers often resulting in micrometastatic spread are epithelial cancers such as prostate cancer, breast cancer and ovarian cancer. These carcinomas metastasize in an organ-specific pattern which most likely depends on mechanical factors, i.e. how the cells are delivered to the organ, as well as compatibility between the tumor cell and the new organ [1]. The epithelial cancers cause the majority of cancer related deaths in western industrialized countries, and the reason for this is early metastasis, which is often occult at the time of diagnosis [3].

1.2 Radioimmunotherapy

Radioimmunotherapy (RIT) is a form of targeted therapy. Targeted therapy, or “magic bullets”, was already envisaged by Paul Ehrlich in the early 1900s, and has today been realized and implemented to some extent [4]. The advantage of targeted cancer therapy is that occult cancer disease (e.g. micrometastases) can be treated, and that normal healthy tissue can be spared from negative side-effects.

In general, RIT is intended to be given as an adjuvant treatment after larger tumors are removed and only minimal residual disease remains. RIT has two main components: 1.) a tumor-specific antibody or antibody fragment and 2.) a radionuclide. The first experiments with radiolabeled antibodies were performed in the 1950's [5, 6] but it was not until around 1980 that studies surrounding the targeting of human tumor-associated antigens were successful in patients [7, 8]. Since then, a

substantial amount of preclinical and clinical studies have been performed [9, 10]. In RIT, the antibody or antibody fragment is injected into the patient to target and bind to the tumor cells. Unlabeled tumor-specific antibodies can be administered as an adjuvant standalone treatment (immunotherapy) and can have a tumor-preventing effect [11, 12]; however, this effect is in many cases not enough to eradicate all tumor cells. Thus, in RIT, cytotoxic radionuclides are attached to the antibodies to enhance the therapeutic efficacy. The radiolabeled antibody conjugates in RIT can be administered in different ways depending on the nature of the disease, for example systemically or intracompartmental/intracavitary [13]. Intracompartmental and intracavitary treatments are given when the metastases primarily have a local spread, and in these cases the targeting time is often relatively short. However, when RIT is given systemically, the targeting time can be long, depending on the location of the tumor cells. The long targeting time can be an obstacle in a systemic treatment, especially when using short-lived radionuclides.

1.3 Pretargeted radioimmunotherapy

Pretargeted radioimmunotherapy (PRIT) is a further advancement of conventional RIT. Since antibodies are large molecules of about 150 kDa, they have a slow in vivo distribution, meaning it can take several hours for them to localize the tumor cells. In PRIT, the treatment is divided into two or three steps [14, 15]. First, an antibody conjugate, called the pretargeting molecule, is injected. When an optimum amount of pretargeting molecule is bound to the tumors, a clearing agent can be administered, which removes the unbound pretargeting molecules from the blood circulation. Subsequently, a small radiolabeled molecule, called the effector, is injected. The effector should have a very high affinity for the pretargeting molecule, and this high affinity combined with the small molecular size of the effector leads to much faster targeting time than can be achieved by the antibody conjugates in conventional RIT. For this reason, PRIT is often superior to RIT, especially when using short-lived radionuclides. The radioactivity uptake in normal tissue is much lower in PRIT, which can lead to an expansion of the therapeutic

window for PRIT compared with RIT. The principle of pretargeting is illustrated in Figure 1.

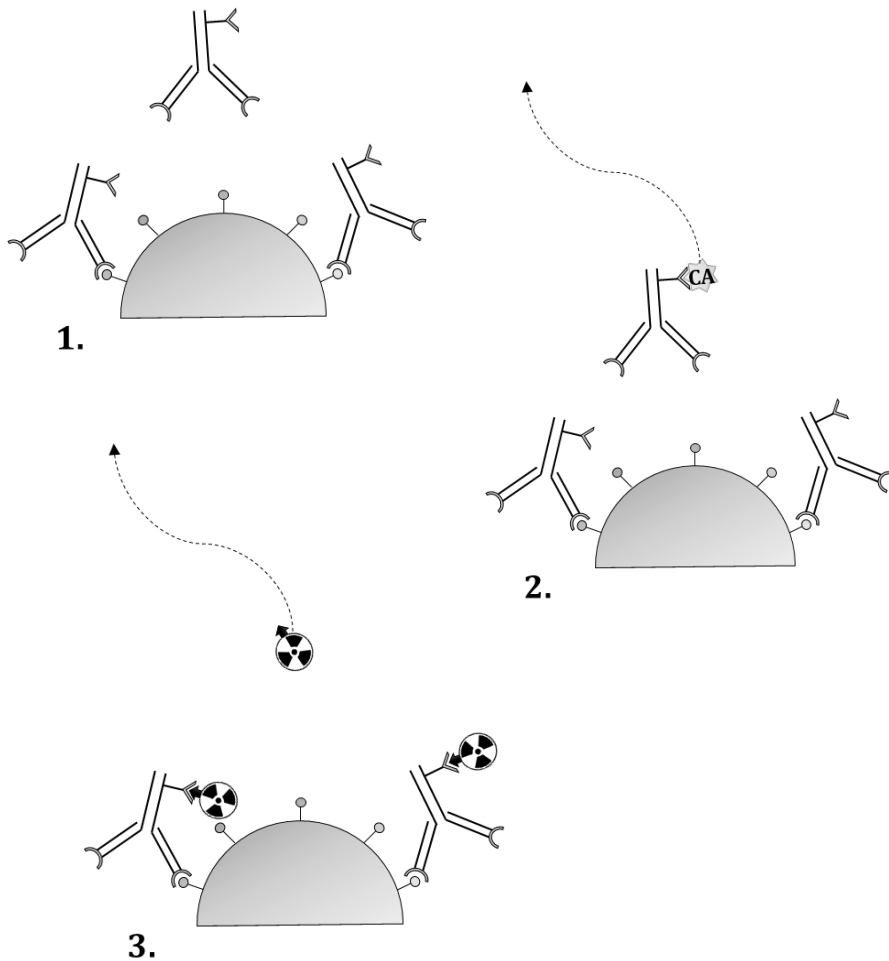


Figure 1. Schematic illustration of pretargeted radioimmunotherapy. 1.) The Y-shaped antibody conjugates (pretargeting molecules) are initially administered to target and bind to the antigenic sites on the tumor cells. 2.) Unbound pretargeting molecules are cleared from the blood, either spontaneously or with the guidance from a clearing agent (CA). 3.) The radiolabeled effectors are administered, which attach to the pretargeting molecules. The small size of the effector facilitates rapid tumor uptake and fast blood clearance to avoid irradiation of normal tissue. Illustration: Anna Gustafsson-Lutz and John Apelgren.

The idea of separating the radionuclide from the antibody was first introduced in 1985 by Reardan et al. [16]. They suggested that antibodies could be produced to be both tumor-specific and have high affinity for the metal chelate indium-EDTA. Shortly after, the pretargeting concept was initiated by Goodwin et al., and they studied monoclonal antibodies (mAbs) with high specificity for derivatives of ^{111}In EDTA for tumor imaging in mice [17, 18]. The theory used in these experiments corresponds to the current pretargeting approach of bispecific antibodies which has been used in multiple experiments [14, 19-21]. The concept of pretargeting with bispecific antibodies is described in more detail below.

There are several existing pretargeting systems, with different approaches for achieving a high affinity between the pretargeting molecule and the effector. The most common approach thus far is to use (strept)avidin and biotin [22, 23]. The bond between avidin and biotin is the strongest non-covalent bond known, with a dissociation constant (K_d) of 10^{-15} M. In most pretargeting systems, avidin or streptavidin is incorporated in the pretargeting molecule, and biotin in the effector. In 1987, Hnatowich et al. studied the (strept)avidin-biotin system and investigated both (strept)avidin-conjugated antibodies and biotin-linked effectors as well as biotinylated antibodies and radiolabeled (strept)avidin [24]. In 1995, pharmacokinetic models were used by Sung and van Osdol to investigate the optimum strategy using (strept)avidin and biotin in the pretargeting system. They concluded that (strept)avidin-conjugated antibodies and biotin-linked radionuclides were preferable to biotin-conjugated antibodies and radiolabeled (strept)avidin [25].

Avidin is a glycosylated protein with a molecular weight of 66 kDa, and streptavidin is a non-glycosylated analog of avidin with a molecular weight of 60 kDa. Both avidin and streptavidin have four binding sites for biotin. However, streptavidin is preferable in a pretargeting system *in vivo* as glycosylated proteins like avidin are rapidly taken up and metabolized by the liver. Biotin is also known as vitamin H (or B₇) and is a water-soluble vitamin. Most people have an intake of 35-70 μg of biotin per day through their diet, and therefore, the level of biotin in the

body could disturb the avidin-biotin system in a therapy. In preclinical studies with PRIT, it is therefore common to implement a biotin-free diet some days before therapy. Biotin is a relatively small molecule with a molecular weight of 0.24 kDa. This favors attachment of biotin to the effector, which should be small to achieve fast blood clearance.

Although the (strept)avidin-biotin system has been the most commonly used for pretargeting, there are other pretargeting systems with high potential. As mentioned previously, systems using bispecific antibodies have been explored in numerous studies. Reardan et al. proposed that bispecific monoclonal antibodies (bsmAbs) could be prepared with one arm having high affinity for a tumor antigen and the other arm deriving from an anti-chelate antibody, since metal chelates were known to have fast and efficient clearance from blood and tissues. In 1989, Le Doussal et al. suggested that by joining two haptens together with a small peptide, uptake and retention would be enhanced within the tumors. This so-called affinity enhancement system (AES) benefits from the higher concentration of bsmAb in the tumor relative to the circulation. The elevated concentration of bsmAb led to a greater interaction of the divalent hapten-peptide over a monovalent form, which then increased the retention in the tumor [26]. This concept has also been confirmed by others [27, 28]. The system used dinitrophenyl as the hapten, but many later studies have instead used the chelate DTPA as the hapten [29-35]. The advantage of using DTPA is that it is also a chelator and can therefore also carry a metal radionuclide.

Yet another pretargeting system uses morpholino-oligonucleotides and complimentary nucleic acid sequences [36, 37]. This system was introduced in 1993 by Kuijpers et al. through hybridization of complimentary DNA fragments used for the binding of radionuclides to pretargeted tumor cells [38]. An antibody oligonucleotide was administered in the first step, followed by a radiolabeled antisense nucleotide in the second step. Improvements have since been implemented in this system in terms of stability and binding affinity, e.g. by the use of morpholino oligomers (MORFs). MORFs are commercially available synthetic DNA analogs, with high specificity towards their complementary MORFs (cMORFs) [39]. An improvement of the system

was demonstrated by He et al. with a multistep procedure in which a molecule incorporating several cMORFs was administered between the MORF-conjugated antibodies and the radiolabeled MORFs [37]. This showed that it is possible to synthesize bivalent MORF effectors and thus bimolecular binding could be achieved, resulting in decreased dissociation and increased affinities for the bivalent MORFs compared to the monovalent forms [40, 41].

Infinite affinity binding is another pretargeting approach, which was initiated in the early 2000s [42]. This concept involves a mutation in the antigen binding site of the antibody, where cysteine residues are introduced. When studying infinite affinity binding, an antibody was developed with specificity for an EDTA chelate for binding to derivatized EDTA ligands. The EDTA has a low affinity for the antibody, but modification of this ligand to enable binding with the introduced cysteine residue results in a permanent covalent bond between the chelate and the antibody [43, 44].

Pretargeting using “click chemistry” has gained more and more interest in the past few years [45-47]. Click chemistry reactions were defined by Sharpless et al. in 2001 [48]. They offer several advantages in pretargeting because they translate well into an in vivo setting, appearing to be completely selective against other chemical species present in a living system. One generally interesting click chemistry reaction is the Huisgen 1,3-dipolar cycloaddition. However, this reaction has very limited use in pretargeting due to the need for a copper (I) catalyst, which is toxic in vivo. Copper-free click chemistry reactions have therefore gained more interest. There are two major types of copper-free reactions: strain-promoted azide-alkyne cycloadditions (SPAAC) [49-52] and inverse electron-demand Diels-Alder (IEDDA) cycloadditions [53]. One example of an IEDDA reaction is the ligation between *trans*-cyclooctene (TCO) and tetrazine (see Figure 2). This is the reaction gaining the most success thus far for implementing in pretargeting due to its extremely high reaction rates (up to $3.8 \times 10^5 \text{ M}^{-1}\text{s}^{-1}$) [54].

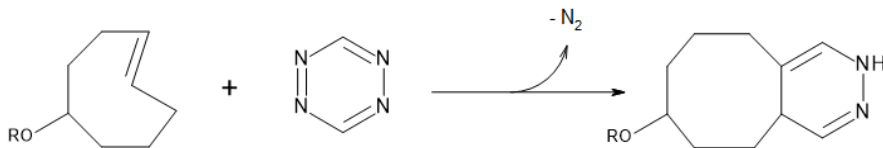


Figure 2. The inverse electron-demand Diels-Alder reaction between TCO and tetrazine.

1.4 Antibodies and antibody-like molecules for RIT and PRIT

Antibodies are also known as immunoglobulins, and are Y-shaped proteins with a molecular weight of ~ 150 kDa. There are five different types of antibodies in humans: IgA, IgD, IgE, IgG and IgM, which are divided according to the structure of their heavy chains. Antibodies are produced by plasma cells and form part of the immune system, as they identify and neutralize cells and viruses perceived as foreign and potentially harmful. The “upper” ends of the Y-shaped antibody include a paratope, which binds to a specific epitope on the antigen.

Around 1975, hybridoma technology was developed, which resulted in an *in vitro* production system for monoclonal antibodies [55]. This technology meant that monoclonal antibodies could be used as targeting vectors in medicine on a much larger scale. Monoclonal antibodies (mAbs) are monospecific antibodies that bind to the same epitope. The first mAbs used for targeted therapy had a murine origin. However, murine antibodies can potentially cause problems in clinical use because of their potential immunogenicity, and they interact poorly with the immune system in patients. A human anti-mouse antibody (HAMA) reaction is common when using murine antibodies, which in the worst case can result in an anaphylactic shock [56]. To circumvent these problems, protein engineering has developed the originally murine mAbs into chimeric, humanized or even fully human mAbs. Furthermore, genetic engineering has facilitated development of other molecules of various sizes with antibody-like properties and sometimes enhanced antigen affinity, such as minibodies (80 kDa) [57] and affibodies (7 kDa) [58]. A smaller molecular size results in faster distribution *in vivo*, which is beneficial for targeting tumor cells.

However, a small-sized molecule has normally a fast blood clearance via the kidneys, which can be disadvantageous for tumor targeting and can result in an elevated radioactivity uptake in the kidneys. Thus, finding an optimum molecular size for every specific application is important.

1.5 The target

Several aspects need to be considered when choosing the proper target in targeted cancer therapy. Overexpression of certain proteins on the cell surface of tumor cells can be exploited for specific targeting with mAbs for example. Ideally, the protein antigen should be highly and homogeneously expressed on the tumor cells, and minimally on the cells of normal tissues. In reality, there is no protein known today that is only highly expressed on tumor cells and not at all in any other tissue. Thus, there is de facto no such thing as truly *tumor-specific* targeting vectors even though this term is often used; a more accurate term would be *tumor-selective* vectors. In addition to specificity, the target protein should not be shedded from the tumor cell, since this means that shedded antigens can react with circulating antibodies and form protein-antibody complexes which may decrease the number of targeting vectors reaching the target cells. Internalization of the targeted protein can potentially be a problem in this type of therapy, especially when using halogenic radionuclides (e.g. astatine or iodine), as halogens after internalization generally leave the cell through exocytosis. Metal radionuclides on the other hand are residualizing, meaning that they remain in the cell after internalization [59].

Suggested target antigens for RIT of lymphomas and leukemias include CD19, CD20, CD22, CD25, CD37, CD45, CD52 and HLA class II [60, 61]. The abbreviation CD stands for “cluster of differentiation” [62] and CD proteins are often receptors or ligands situated on the cell surface. Potential target proteins for ovarian cancer treatment include the folate receptor alpha [63-65], the sodium dependent phosphate transport protein 2b (NaPi2b) [66-68], which is the protein mostly used as the target throughout this thesis, and the human epidermal growth factor receptor 2 (HER2) [69, 70]. There are several subtypes within each type of cancer, and each subtype may have a different antigen expression.

Another important factor for the successful implementation of RIT is to have access to all tumor cells, at least so that they are within the range of the radiation. Tumor growth pattern, vascularization and location of the tumor are thus aspects influencing the probability of curing the disease. Accessibility is the main reason why RIT is primarily suited for smaller tumors, since larger tumors often have compromised vascularization and high interstitial pressure which can hinder diffusion of the therapeutic agent within the tumor tissue.

1.6 Radionuclides for targeted therapy

It is important to find the appropriate radionuclide for every specific therapy. Important properties of the radionuclide are physical half-life, decay chain, decay mode and chemical properties. Sufficient energy from the ionizing radiation has to be deposited in a tumor cell to obtain an adequate therapeutic response. The ionization density of a charged particle through matter is designated by its linear energy transfer (LET). LET is measured in keV/ μm , which means it states the energy deposited per path length unit of an emitted particle. Cell death as a result of irradiation is mainly caused by DNA damage, which can occur either by the irradiation itself, or by indirect effects such as radiation-induced free radicals. Different types of DNA damage can occur following irradiation, for example single strand breaks (SSBs), double strand breaks (DSBs), and multiple damaged sites (MDSs), which involve several types of lesions in close proximity to each other. The DNA can normally be easily repaired from SSBs by repairing systems; however, DSBs and MDSs are more complex and thus more likely to cause cell death. Low-LET radiation is less ionizing, and therefore more prone to result in SSBs, while the amount of DSBs increases with increasing LET (up to approximately 300 keV/ μm). The probability that DSBs rejoin also reduce with increasing ionization density [71].

Factors other than ionization density will also affect cell survival. Dose rate is one example; however, this is mainly important for low-LET irradiation. High dose rate irradiation delivered in short periods of time generally results in a greater biological response [72]. The presence of oxygen is yet another factor that can influence cell survival since it

results in an elevated concentration of free radicals [73]. However, the presence of oxygen is again much more important for low-LET radiation, meaning that high-LET radiation can efficiently kill cells also under hypoxic conditions [74].

Most research in the area of RIT has been carried out with beta (β) particle emitters. However, alpha (α) particle emitters for RIT are gaining increased interest, especially in the past 30 years. In 1986, Humm simulated the absorbed dose for different radionuclides with various radiation qualities applicable in RIT, finding that α -emitting radionuclides would be optimum for the treatment of microscopic tumors [75]. Yet another alternative for targeted radiotherapy is radionuclides emitting auger electrons (although auger electrons damage cells only over a very short range, less than the size of a single cell, possibly making them less useful in RIT). As all therapeutic radiation is toxic not only to tumor cells but also to normal tissue, irradiation of normal tissue should in every way be minimized. In RIT, this can be achieved by utilizing a good targeting vector, having a strong chemical bond between the targeting vector and the radionuclide, and favorable pharmacokinetic properties.

1.7 Beta emitters

Beta (β) particles are electrons or positrons emitted in the decay of certain unstable isotopes. The energy of the β radiation varies from 0.05-2.3 MeV and the path length in tissue is up to around 1 cm [72]. The LET of β particles is around 0.2 keV/ μ m, which is low compared with the LET of α emitters. The most common β emitters used for preclinical and clinical research and therapy are iodine-131 (^{131}I) and yttrium-90 (^{90}Y).

^{131}I has a half-life ($t_{1/2}$) of 8.0 days (d) and a range of 2 mm in tissue. This radionuclide is used extensively in the clinic today, for example in the treatment of thyroid cancer. Iodine naturally accumulates in the thyroid and hence does not need a targeting vector for thyroid cancer treatment. ^{131}I is also used in RIT; an ^{131}I -labeled mAb called tositumomab has been commercially approved for treatment of non-Hodgkin's lymphoma [76].

^{90}Y has a $t_{1/2}$ of 64.1 h and a path length of 12 mm in tissue. The longer range makes ^{90}Y more suitable for slightly larger tumors. However, a side effect of the longer path length is of course more irradiation of healthy tissue, e.g., outside and beyond the target cells. ^{90}Y is used for RIT as well, and a mAb named ibritumomab labeled with ^{90}Y is approved by the U.S. Food and Drug Administration (FDA) for clinical treatment of non-Hodgkin's lymphoma [77].

1.8 Alpha emitters

Alpha (α) particles consist of two protons and two neutrons, i.e. the composition of a helium nucleus. The energy of α radiation varies between 5-9 MeV and the path length is between 40-100 μm in tissue [72]. Consequently, the LET of α particles is 50-230 keV/ μm , i.e. up to more than 1000 times higher than the LET of β particles [74]. Alpha particles thus cause extensive ionization in a short range in matter, leading to very high cytotoxicity along their path lengths. Therefore, they are very useful in eradicating micrometastases and single cancer cells, for example in the treatment of ovarian cancer, lymphoma and hematologic malignancies.

There are only a few α emitters of interest for cancer therapy. Half-life, decay chain, supply and cost are examples of parameters to consider when choosing the proper radionuclide. Alpha emitters used in preclinical and/or clinical research are e.g. actinium-225 (^{225}Ac), astatine-211 (^{211}At), bismuth-212 (^{212}Bi), bismuth-213 (^{213}Bi), radium-223 (^{223}Ra), radium-224 (^{224}Ra), thorium-226 (^{226}Th) and thorium-227 (^{227}Th) [78]. A number of these (^{225}Ac , ^{223}Ra , ^{224}Ra , ^{226}Th and ^{227}Th) have several α emitting daughter nuclides with long half-lives which can possibly decay far outside the target and thereby lead to toxicity in vivo.

This thesis focuses on two of the α emitters mentioned above: ^{213}Bi and ^{211}At . These radionuclides have half-lives of 45.6 min and 7.21 h, respectively. Both nuclides decay with 100 % α emission, either directly or through α -emitting daughter nuclides with very short half-lives, contributing to their suitability for therapy [79]. ^{213}Bi can be produced by a generator containing ^{225}Ac , which makes ^{213}Bi readily accessible

although the half-life is very short [80]. ^{211}At is cyclotron-produced by a medium energy cyclotron [81]; thus, therapy with ^{211}At requires certain proximity between the patient and the cyclotron due to the relatively short half-life. ^{213}Bi and ^{211}At both also emit gamma (γ) radiation in their total decays, which makes radioactivity determination with a gamma counter and imaging with a gamma camera feasible.

2 AIMS

The overall aim of this PhD project was to develop and evaluate molecules for RIT and PRIT, using the α emitting radionuclides ^{213}Bi and ^{211}At . In the studies performed, the synthesized molecules have been evaluated in vitro and in some cases in vivo. The in vivo studies were performed in a mouse model and focused on biodistribution and/or therapeutic efficacy.

The specific aims of the studies included in this thesis were:

- Paper I: to compare the biodistribution and the therapeutic efficacy of ^{213}Bi - and ^{211}At -labeled antibodies (MX35) in an ovarian cancer mouse model.
- Paper II: to compare the therapeutic efficacy of different injected activity levels of ^{213}Bi -labeled MX35 in the same ovarian cancer model as in Paper I.
- Paper III: to produce and evaluate ^{211}At -labeled immunoconjugates with *N*-[2-(maleimido)ethyl]-3-(trimethylstannyl)benzamide in vitro and in vivo.
- Paper IV: to synthesize and evaluate polylysine-based effectors for PRIT and pretargeted radioimmunoimaging (PRII). These effectors were constructed for labeling with metal radionuclides such as ^{213}Bi .
- Paper V: to synthesize and evaluate polylysine-based clearing agents for pretargeting, for clearing the blood from unbound pretargeting molecules in vivo.

3 BACKGROUND

3.1 Bismuth-213

Bismuth (Bi) is a metallic element with the atomic number 83. ^{213}Bi decays with a half-life of 45.6 min and has 100% α emission in its total decay. Ninety-eight percent of the ^{213}Bi decays first with β^- emission to ^{213}Po , which decays with α emission to ^{209}Pb with a $t_{1/2}$ of 4.2 μs . Two percent of the ^{213}Bi decays with α emission to ^{209}Tl , which in turn decays with β^- emission to ^{209}Pb . ^{209}Pb is a β^- emitter that decays with a $t_{1/2}$ of 3.3 h.

3.2 The $^{225}\text{Ac}/^{213}\text{Bi}$ generator

The ^{213}Bi used throughout this work was eluted from $^{225}\text{Ac}/^{213}\text{Bi}$ generators which were produced at the Institute for Transuranium Elements (ITU) in Karlsruhe, Germany. The ^{225}Ac that is used for the generators is obtained from the decay of ^{229}Th . There are only two sources in the world for the production of clinically relevant amounts of ^{225}Ac ; one is located at ITU in Karlsruhe and the other at the Oak Ridge National Laboratory, Oak Ridge, TN, USA. The ^{229}Th is isolated from mixed waste material from the production of ^{233}U at the Oak Ridge National Laboratory. The ^{225}Ac is then separated from ^{229}Th through ion exchange and extraction chromatography methods [80, 82].

The $^{225}\text{Ac}/^{213}\text{Bi}$ generator consists of a cation exchange column (Dowex AG-MP-50, 100-200 mesh) which is loaded with ^{225}Ac in HNO_3 and then converted into Cl^- form using HCl . To elute the ^{213}Bi from the generator column for subsequent labeling of antibodies, peptides and other molecules, a solution of 0.1 M $\text{NaI}/0.1$ M HCl is run through the column. The yield for the eluted ^{213}Bi is normally around 90% [80, 83].

The decay chain of ^{225}Ac is shown in Figure 3.

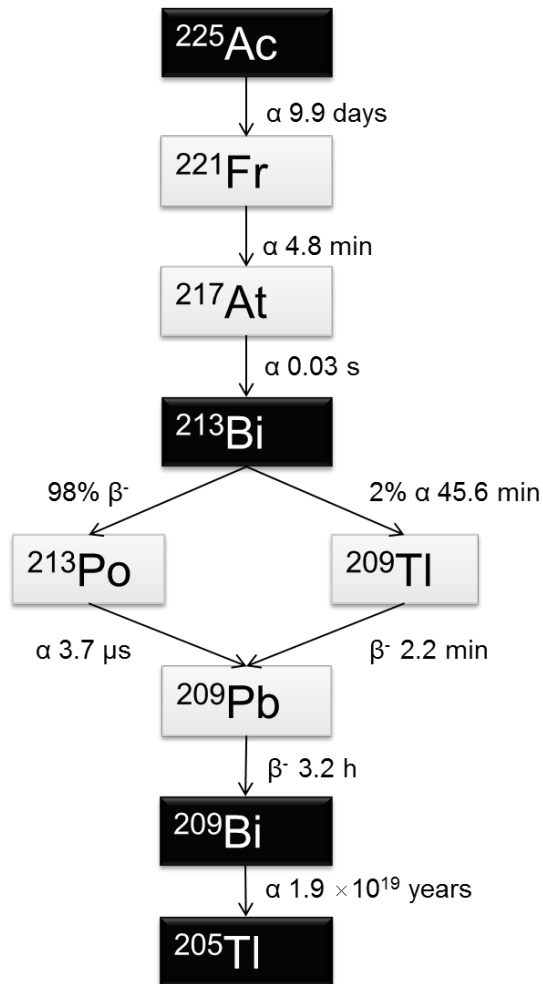


Figure 3. Decay chain of the $^{225}\text{Ac}/^{213}\text{Bi}$ generator, with indicated decay modes and half-lives of the radionuclides.

3.3 Radiolabeling with ^{213}Bi

The ^{213}Bi is eluted from the $^{213}\text{Bi}/^{225}\text{Ac}$ generator probably as $\text{BiI}_4^-/^{213}\text{BiI}_5^{2-}$ [84]. ^{213}Bi is a heavy metal with the oxidation number (III), and is easily chelated by common chelators such as 2-[bis[2-[bis(carboxymethyl)amino]ethyl]amino]acetic acid (DTPA) and derivatives thereof (e.g., the bifunctional *N*-[(*R*)-2-amino-3-(*p*-isothiocyanato-phenyl) propyl]-*trans*-(*S,S*)-cyclohexane-1,2-diamine-*N,N,N',N'',N'''*-pentaacetic acid, also called CHX-A''-DTPA), or 1,4,7,10-tetraazacyclododecane-1,4,7,10-tetraacetic acid (DOTA). Throughout the studies of this thesis, radiolabeling with ^{213}Bi was performed by chelation with either CHX-A''-DTPA or a DOTA derivative. The CHX-A''-DTPA had an isothiocyanyl (SCN-) group which makes it an amine reactive bifunctional chelator, and is therefore attachable to the ϵ -amine of the lysine residues of antibodies or peptides. The DOTA derivative used throughout the studies of this thesis was the bifunctional *p*-SCN-Bn-DOTA, which is amine reactive in the same way as the CHX-A''-DTPA.

Because of the short half-life of ^{213}Bi , short labeling times and high radiochemical yields (RCY) are important to have a sufficient amount of the initial ^{213}Bi activity left in the final product. The labeling reaction throughout this work was performed in 0.1 M citrate buffer, pH \sim 5.5, typically rendering an RCY of 50-60% and a radiochemical purity (RCP) of 95%. All solutions and equipment were kept as metal free as possible to prevent contamination of other metals in the labeling reaction. When labeling CHX-A''-DTPA-bound molecules, the labeling reaction time was 5 min at room temperature (RT), and when labeling DOTA-conjugated molecules, the reaction time was 5 min at 95°C in a water bath.

3.4 Astatine-211

Astatine (At) is the heaviest element of all halogens, and has the atomic number 85. It is a very rare element and only occurs as short-lived radioactive isotopes. ^{211}At has a $t_{1/2}$ of 7.21 h and decays to 58 % through electron capture (EC) to ^{211}Po . ^{211}Po in turn decays with a $t_{1/2}$ of 0.52 s through α emission to the stable isotope ^{207}Pb . Forty-two percent of the ^{211}At disintegrates with α emission to ^{207}Bi , which in turn decays

through EC to ^{207}Pb with a $t_{1/2}$ of 38 years. The decay chain of ^{211}At is illustrated in Figure 4.

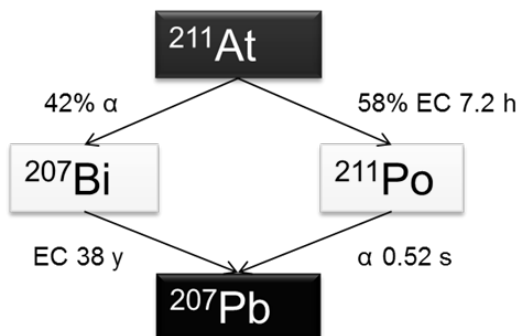
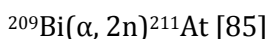


Figure 4. The decay of ^{211}At , with indicated decay modes and half-lives of the radionuclides.

3.5 Production and distillation of ^{211}At

The most common way of producing ^{211}At is in a cyclotron through the nuclear reaction:



The ^{211}At used in the studies of this thesis was cyclotron produced at the PET and Cyclotron Unit at Rigshospitalet in Copenhagen, Denmark, by irradiating a bismuth-209 (^{209}Bi) target for 4-8 h with α particles of 28 MeV and a beam current of $\sim 18 \mu\text{A}$.

The cyclotron-produced $^{211}\text{At}(\text{s})$ has to be isolated from the irradiated target and transformed into a chemically reactive form suitable for labeling. This can be done either by dry distillation [86, 87], or by chemical extraction through acid treatment of the target (the “wet chemistry” approach) [88]. In the current studies, the solid ^{211}At was mechanically removed from the target and then dry-distilled. The ^{211}At was transferred to a quartz tube, which was inserted into a furnace preheated to a temperature of approximately 670°C . The vaporized ^{211}At

was then transferred by reduced pressure to a cooled (-77°C) capillary loop, where it was trapped by condensation. Subsequently, the ^{211}At was rinsed from the capillary loop by a small volume of chloroform (CHCl_3). The CHCl_3 was thereafter evaporated and the ^{211}At could be dissolved in an appropriate labeling solution.

3.6 Radiolabeling with ^{211}At

Being a halogen, astatine shares many chemical properties with the other halogens, e.g. iodine. However, labeling proteins with radioactive iodine can be performed by so-called “direct labeling” through connecting oxidized nuclide (I^+) to the amino acid tyrosine. The iodine-tyrosine bond is stable in vitro and reasonably stable in vivo. Direct labeling in the case of astatine can only be done with a low reaction yield and results in a weak bond [89], due to other preferred oxidation states of astatine than of iodine. Astatine has been shown to have more metallic properties than the other halogens, and therefore, chelation attempts have been performed with DOTA for example [78]. Although results have been somewhat successful, it is unclear if this approach can have any application for medical research.

Another approach for labeling with ^{211}At is to use boron-containing molecules. Wilbur et al. have for example synthesized a *closo*-decarborate(2-) cage which enables direct astatination with high labeling yields and a low deastatination rate in vitro and in vivo [90, 91]. However, some activity uptake has been shown in the liver and intestine [92].

The most common approach in ^{211}At -labeling thus far has been to use so-called “activated tin ester” (ATE) derivatives [93-95]. The tin-carbon bond has suitable properties for halogen substitution. This approach is very fast and demonstrates high labeling yields, and therefore, it is this approach that was used in the ^{211}At -labelings performed. *N*-succinimidyl-3-(trimethylstannyl)benzoate (*m*-MeATE) was connected to proteins or peptides via the ϵ -amino group of their lysine residues. In the labelings with ^{211}At throughout this study, the ^{211}At was oxidated using a small amount of *N*-iodosuccinimide (NIS) and then mixed with

an *m*-MeATE-conjugated antibody or peptide in a buffer with a pH of ~ 5.5 . The labeling reaction was allowed to proceed for approximately 1 min at RT, typically rendering an RCY of 70-80% and an RCP of $>95\%$. Subsequently, more NIS was added to substitute the residual tin groups of the *m*-MeATE with iodine to avoid injecting the toxic tin.

3.7 Ovarian cancer

Ovarian cancer is diagnosed in 1-2% of women and includes various cancers originating from the ovarian cells. The most common form of ovarian cancer emerges from the epithelial cells of the ovaries. The prognosis is often poor due to late diagnosis, which is generally a consequence of late and unspecific symptoms. The majority of patients have already reached stage III at the time of diagnosis, with metastases in the peritoneal cavity and on the peritoneal lining, and only 45 % of patients have a 5-year relative chance of survival [96]. Despite seemingly successful treatments involving surgery and chemotherapy, around 70 % of patients will suffer from recurrence. The tumors most often recur primarily within the peritoneal cavity, and production of ascites and bowel obstruction often occurs prior to death. Since the recurrence generally occurs within the peritoneal cavity, an intraperitoneal adjuvant treatment is feasible after the conventional treatment is completed. At this point in time, laparoscopic complete remission should have been achieved; thus, possible residual disease is minimal and consists only of micrometastases. Consequently, RIT using an α emitter such as ^{211}At or ^{213}Bi has the potential to be highly beneficial for this type of adjuvant treatment. Indeed, several preclinical studies of ^{211}At -RIT have demonstrated therapeutic potential [97-104], leading up to a phase I clinical trial [105, 106]. In this clinical trial, 12 women received ^{211}At -RIT after chemotherapy following intraperitoneal relapse. Pharmacokinetic and dosimetric data [107], as well as lack of observable side effects by patients and physicians, have indicated further potential for ^{211}At -RIT as an adjuvant treatment of ovarian cancer.

3.8 Ovarian cancer tumor model

The *in vivo* experiments in this thesis involving therapeutic efficacy studies or tumor uptake have been performed in immunodeficient BALB/c (nu/nu) mice. The mice were inoculated with the human epithelial ovarian carcinoma cells NIH:OVCAR-3 (National Institute of Health Ovarian Carcinoma Cell Line 3). The cell line was obtained from the American Type Culture Collection (ATCC; Rockville, MD, USA). The NIH:OVCAR-3 cells overexpress the sodium-dependent phosphate transport protein 2b (NaPi2b), which was used as the target for the therapies. The NaPi2b is overexpressed on a number of epithelial cancer cell lines, and approximately 1.2×10^6 copies of this protein exist the cell surface of NIH:OVCAR-3 [108]. When these cells are inoculated intraperitoneally in BALB/c (nu/nu) mice, the tumor growth mimics the patient situation well, with peritoneal metastases and ascites production [109].

3.9 Antibodies for ovarian cancer targeting

One mAb which has been developed to target the protein NaPi2b on the ovarian cancer cells is MX35. This is a murine antibody, developed by immunization of mice with ovarian carcinoma specimens at the Memorial Sloan-Kettering Cancer Center (New York, NY, USA) [110, 111]. It has shown homogenous reactivity with ~90 % of human epithelial ovarian cancer cells, but reacts to a small extent with normal tissues [66]. The mAb MX35 was used in the studies described in Papers I-III, and was produced from hybridoma cells provided by the Ludwig Institute of Cancer Research, Zürich, Switzerland.

Another antibody used in preclinical RIT evaluations of ovarian cancer is trastuzumab (Roche, Basel, Switzerland), and this antibody was used for some of the *in vitro* studies in Paper III. This mAb is commercially available under the name Herceptin and recognizes the HER2 protein. HER2 is mainly overexpressed on breast cancer tumors (approximately 15-30% of breast cancers [112, 113]), and therefore, unlabeled trastuzumab is used in adjuvant treatment of metastatic breast cancer [114, 115]. In addition to breast cancer tumor cells, the HER2 protein is

also overexpressed in for example ovarian-, stomach-, and some forms of uterine cancer [116, 117].

4 METHODS

4.1 The chemistry of conventional radioimmunotherapy with ^{213}Bi and ^{211}At (Papers I-III)

In Papers I and II, the ^{213}Bi -labeling of the MX35 antibody was performed using the bifunctional chelator CHX-A''-DTPA. The antibody was reacted with 15 times molar excess of chelator overnight in 0.2 M carbonate buffer, pH 8.5, rendering on average two available chelators on every antibody. The conjugation of the antibody with CHX-A''-DTPA is illustrated in Figure 5.

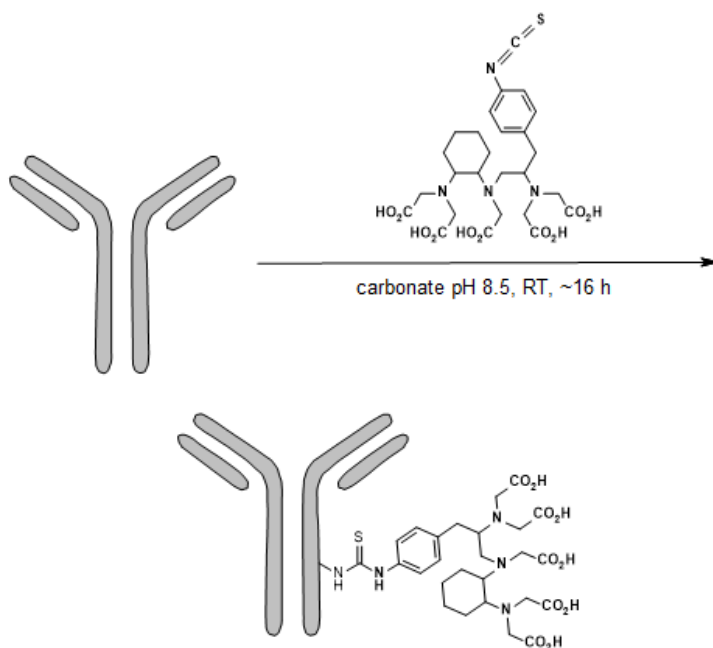


Figure 5. Conjugation of an antibody with CHX-A''-DTPA.

In Papers I and III, antibodies were labeled with ^{211}At . In advance to the radiochemistry, an immunoconjugate was produced with the lysine-reactive intermediate reagent *N*-succinimidyl-3-(trimethylstannyl)benzoate (*m*-MeATE) for subsequent direct labeling

with ^{211}At . This procedure was used in both Papers I and III. For the conjugation, the antibody was reacted with a 7.5 fold molar excess of the *m*-MeATE reagent for 30 min in 0.2 M carbonate buffer, pH 8.5, yielding an average of approximately 7 linkers per antibody. However, in Paper III, a new coupling reagent named *N*-[2-(maleimido)ethyl]-3-(trimethylstannyl)benzamide (MSB) was also used, which reacts selectively with the unsubstituted sulphhydryl groups from gently reduced disulphide bridges of the antibody [118]. In this way, the coupling reagent is site-selectively positioned on the immunoconjugate, at a distance from the antigen-binding sites. In contrast to this new reagent, the amine-reactive *m*-MeATE reacts with the lysines on the antibody and is therefore distributed more randomly. Thus, it could disturb the immunoreactivity if bound in proximity to the antigen-binding sites. When conjugating with the MSB reagents, the antibody was first reduced by 1,4-dithiothreitol (DTT) to open the disulphide bridges, and then reacted for 45 min with a 10 fold molar excess of MSB reagent, rendering on average approximately 6 linkers per antibody. The conjugation of an antibody with MSB is illustrated in Figure 6.

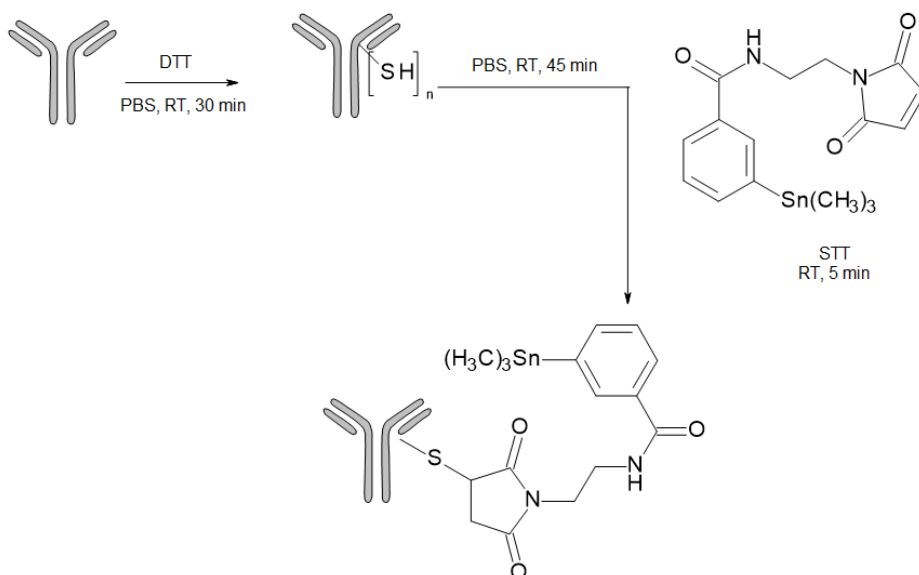


Figure 6. Reduction and MSB-conjugation of an antibody.

4.2 The chemistry of the synthesized pretargeting agents (Papers IV and V)

The (strept)avidin-biotin pretargeting system was used for all pretargeting agents in this thesis. This system was chosen as it is well-tested and has been used for a long time by our group. In Paper IV, effector molecules for pretargeting were synthesized. The novelty in this effector synthesis was to use a polylysine scaffold for reaction with biotin and bifunctional chelators. Due to the polylysine backbone, the effector can easily be modified in size and charge. The amount of biotin and bifunctional chelator incorporated in the effector can also be readily varied due to the number of accessible amino groups of the polylysine. To synthesize the effector, polylysine was reacted with a 5 fold molar excess of biotin for 30 min in 0.2 M carbonate buffer, pH 8.5, and then with different amounts of bifunctional chelator (CHX-A''-DTPA or *p*-SCN-Bn-DOTA) overnight in the same buffer. The effector was subsequently charge-modified by succinic anhydride. The effector syntheses with the different chelators are illustrated in Figure 7 and Figure 8.

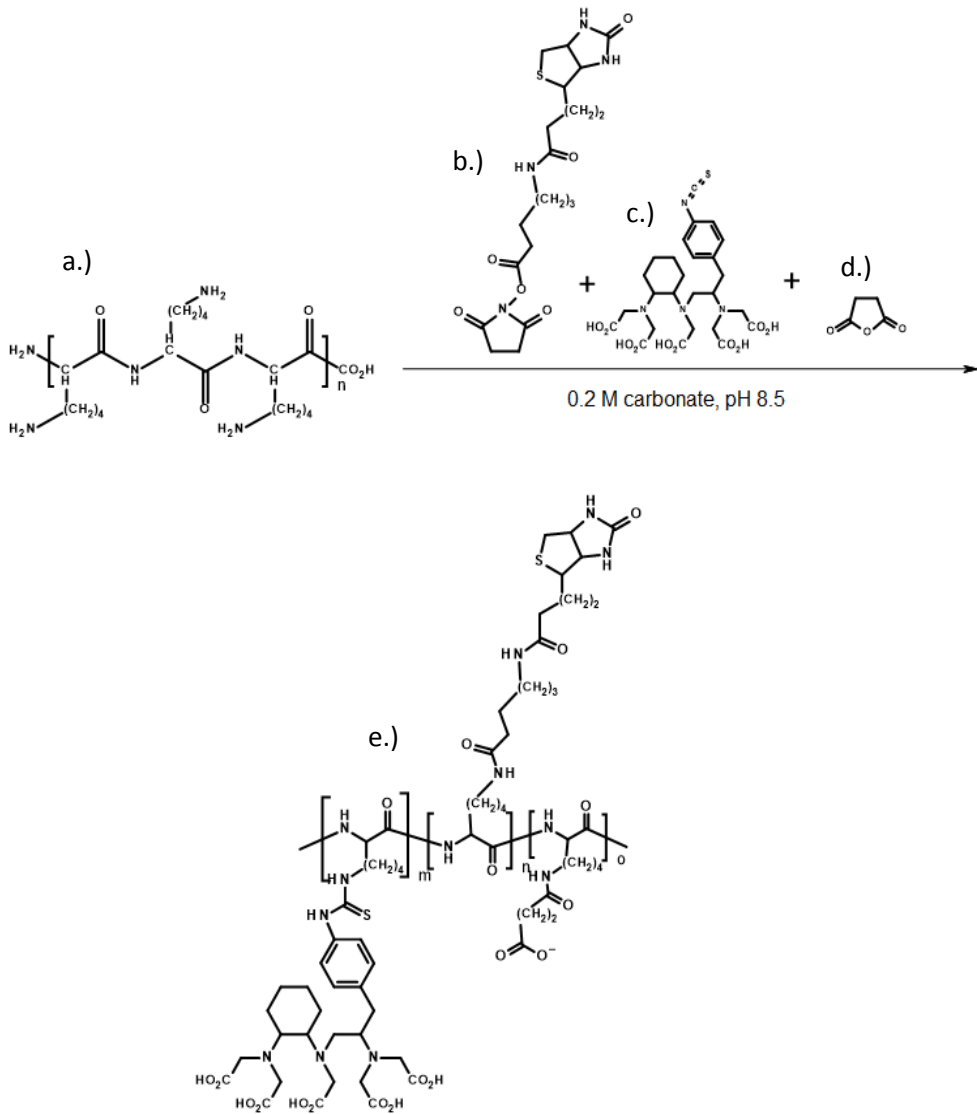


Figure 7. Synthesis of CHX-A'-DTPA-conjugated effector. Poly-L-lysine (a.) is reacted with NHS-LC-biotin (b.) and CHX-A'-DTPA (c.), and subsequently charge-modified with succinic anhydride (d.) to produce the effector (e.).

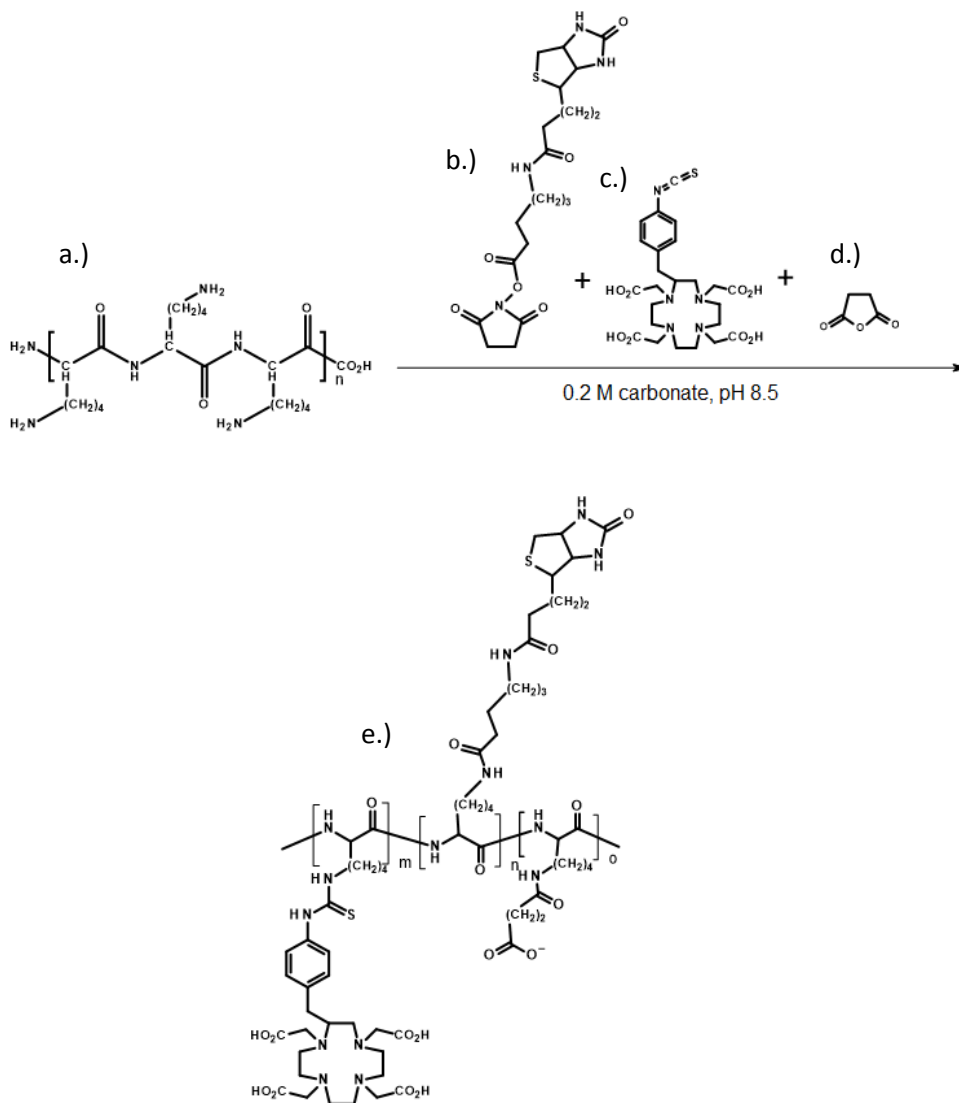


Figure 8. Synthesis of the DOTA-conjugated effector. Poly-L-lysine (a.) is reacted with NHS-LC-biotin (b.) and p-SCN-Bn-DOTA (c.), and subsequently charge-modified with succinic anhydride (d.) to produce the effector (e.).

In Paper V, a polylysine-based clearing agent for pretargeting was synthesized. As with the polylysine-based effectors, this clearing agent can easily be varied in size, charge and composition, which simplifies the optimization of the function of the clearing agent. In the synthesis, polylysine was reacted with a 10 fold molar excess of biotin for 30 min in 0.2 M carbonate buffer, pH 8.5, and then with a 20 fold molar excess of sulfo-NHS-phosphine for 30 min in the same buffer. Thereafter, the molecule was reacted overnight with a 30 fold excess of *N*-azidoacetylgalactosamine which attaches to the phosphine via the Staudinger reaction. Subsequently, the molecule was charge-modified with succinic anhydride. The clearing agent synthesis is illustrated in Figure 9.

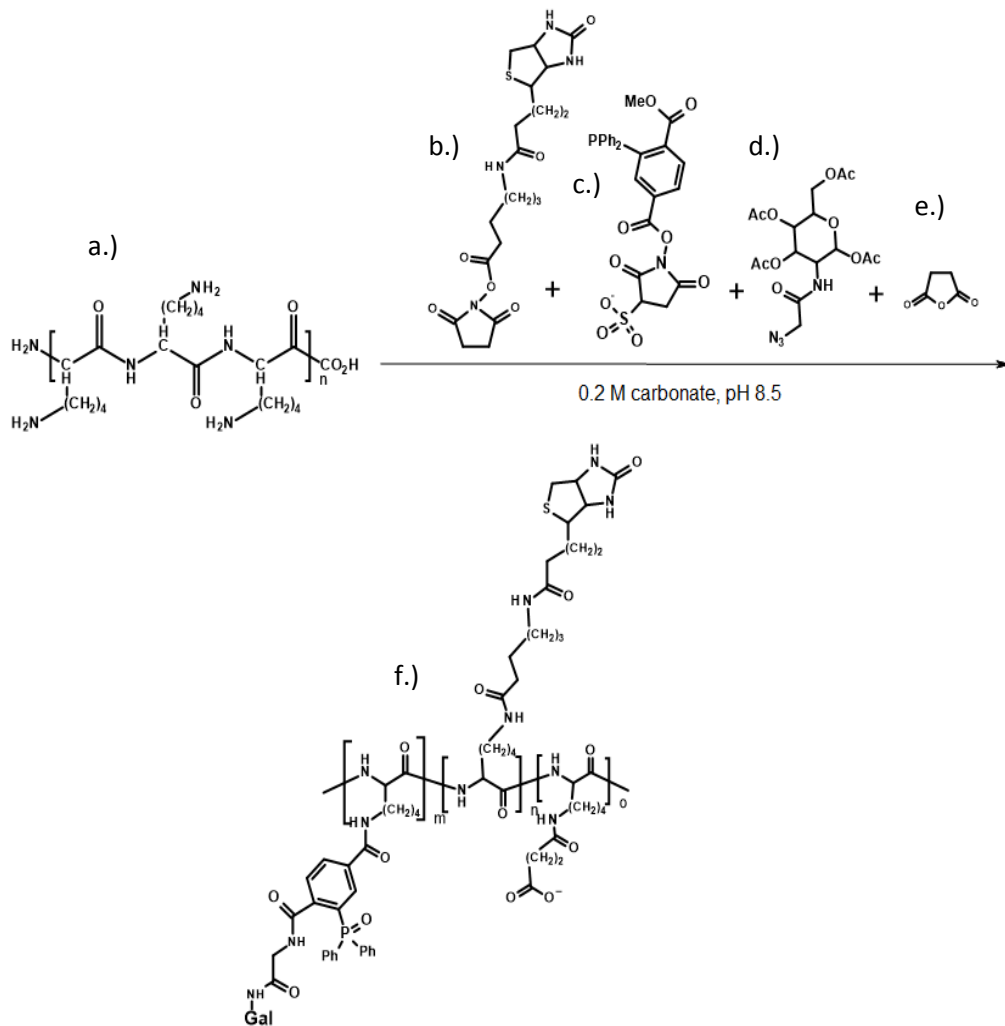


Figure 9. Synthesis of the polylysine-based clearing agent. Poly-L-lysine (a.) is reacted with NHS-LC-biotin (b.), sulfo-NHS-phosphine (c.) and tetraacetylated N-azidoacetyl galactosamine (d.). The molecule is also charge-modified with succinic anhydride (e.) to finalize the clearing agent (f.).

4.3 In vitro analyses

4.3.1 *Molecular structure analysis*

With the methods chosen to produce the immunoconjugates (Papers I-III), it is not possible to synthesize one defined molecule. The amine-reactive linkers can react with any of the available lysine residues of the antibody, rendering a random conjugation as the lysine residues are unsystematically distributed over the antibody structure. When using a sulphur reactive reagent like MSB (Paper III) it reacts site-specifically [119]; however, the amount of linkers per antibody can still not be defined precisely. Therefore, analysis methods will give information about the average number of coupling agents that are attached to each antibody. The chelated antibody in Papers I and II was analyzed by an arsenazo III spectrophotometric assay [120] to evaluate the average number of available chelators bound to the antibody. In Paper III, the amount of amine reactive linkers attached to the antibody was evaluated using 2,4,6-trinitrobenzene sulfonic acid (TNBS), and the amount of sulphur reactive linkers was analyzed by evaluating the tin (^{118}Sn) content using Thermo Scientific Thermo ICAP-Q ICP-MS. To investigate if the antibody structures were intact after conjugation and labeling, fast protein liquid chromatography (FPLC) analyses were performed.

The effectors in Paper IV were analyzed for molecular composition and structure using three different methods. The amount of attached biotin on each effector was analyzed using TNBS, the amount of chelator through the arsenazo III spectrophotometric assay, and, finally, the degree of succinylation using TNBS. The purity of the final product was analyzed using FPLC.

4.3.2 *Radiochemical purity*

The radiochemical purity (RCP) is defined as the ratio between the radioactivity of the element in the desired chemical form and the total radioactivity of the same element in all present chemical forms [121]. In general, all molecules labeled with metallic radionuclides (e.g., ^{213}Bi) were tested for RCP using instant thin-layer chromatography (ITLC)

using 0.1 M citrate, pH 5.5, as mobile phase. The molecules labeled with ^{211}At were analyzed for RCP using methanol precipitation and the ^{125}I -labeled molecules using trichloroacetic acid precipitation.

4.3.3 *Cell binding (Papers I-III)*

The cell binding of the labeled antibodies in Paper I-III was analyzed in vitro. 10 ng of the radioimmunoconjugates was added to duplicates of 0.5 ml of cell suspension with different cell concentrations (maximum 5×10^6 cells/ml). The samples were incubated for 2-3 h with vigorous agitation. Subsequently, they were centrifuged at $1438 \times g$ for 5 min, and the supernatant was removed from the cell pellets. The cells were washed with 1 ml of PBS, centrifuged again, and the supernatant was removed. The cells were measured in a γ counter and compared with reference solutions containing 10 ng of radioimmunoconjugate to evaluate the ratio of bound activity/total applied activity (B/T).

4.3.4 *Avidin binding (Paper IV)*

Avidin-linked agarose beads (50 μl ; Thermo Fisher Scientific, Rockford, IL, USA) were added to 3 microcentrifuge filter tubes (Corning Costar Spin-X; Sigma-Aldrich Sweden AB, Stockholm, Sweden). The tubes were centrifuged for 1 min at $503 \times g$, and 100 μl of PBS and 30 ng of labeled effector were subsequently added to the filter tubes. As reference samples, 100 μl of PBS were added to 3 empty filter tubes. All samples were incubated for 1 h at RT with gentle agitation. The filter tubes were then centrifuged for 1 min at $503 \times g$, and the filters were washed twice with PBS. The filters were removed from the tubes and measured in a γ counter (Wizard 1480, Wallac, Finland). The avidin binding capacities of the effector molecules were calculated as bead-associated activity divided by total applied activity.

4.4 **Animal experiments**

All animal experiments were performed in BALB/c (nu/nu) mice, except for the animal experiment in Paper V which was performed in normal BALB/c mice. The in vivo experiments were all approved by the ethics committee of the University of Gothenburg.

4.4.1 *Therapeutic efficacy and toxicity of α -RIT in the ovarian cancer model (Papers I and II)*

Therapeutic efficacy was evaluated in tumor-bearing BALB/c (nu/nu) mice, which served as an ovarian cancer tumor model. The mice were intraperitoneally inoculated with 1×10^7 OVCAR-3 cells, and tumors were allowed to grow for 2-4 weeks. Prior to the therapeutic injections, the animals were divided into groups of 20 individuals. In Paper I, the animals were given 3 MBq of ^{213}Bi -MX35, 0.4-0.5 MBq of ^{211}At -MX35, or PBS as a reference treatment. The activities administered were chosen to result in equal absorbed doses to the peritoneum in a human patient. In Paper II, 3 MBq or 9 MBq of ^{213}Bi -MX35 were administered, or unlabeled MX35 as a reference treatment. The mice in both studies were weighed every 7-10 days, and white blood cell (WBC) counts were monitored in the blood of the mice up to 14 days following treatment. After 8 weeks, the mice were sacrificed and presence of tumors and/or ascites was investigated. Tissues from the abdominal wall and mesentery (and spleen in Paper II) were taken for paraffin sectioning and hematoxylin and eosin (H&E) staining to check for microscopic tumors. In Paper II, tissue sections were extracted from the tissue samples with an interval of 50-100 μm , while the analysis was somewhat less extensive in Paper I. In Paper II, the accuracy of defining presence/absence of tumor cells in the H&E stained sections was confirmed using MX35 mAbs and peroxidase immunohistochemistry (IHC) in uncertain cases.

4.4.2 *Biodistribution studies (Papers I, III-V)*

In all biodistribution studies, selected organs were dissected from the mice, weighed and analyzed for radioactivity uptake using a γ counter. Subsequently, the percentage of the injected dose per gram (%ID/g) in the organs was evaluated. In Paper I, the biodistribution studies were performed for the intraperitoneally injected radioimmunoconjugates in tumor-free BALB/c (nu/nu) mice. The distribution of the immunoconjugates in interesting organs was analyzed in mice sacrificed 15 min, 45 min, 90 min and 180 min post injection, i.e. when up to 94% of the ^{213}Bi had decayed. In Paper III, the biodistribution study was performed in tumor-bearing BALB/c (nu/nu) mice to compare tumor

and normal tissue uptakes of ATE- and MSB-conjugated antibodies. The mice were subcutaneously inoculated with 1×10^7 OVCAR-3 cells through double-sided injection in the scapular region. After 4 weeks, when tumors had established, the animals were systemically administered with the ^{211}At -labeled immunoconjugates. Distribution in tumors and normal tissues was analyzed 1 h, 5 h and 25 h post injection. In Paper IV, a renal uptake study was performed in BALB/c (nu/nu) mice with two different sizes of the ^{213}Bi -labeled effector molecule. The radioactivity uptake in the kidney was monitored in mice sacrificed 15 min, 45 min, 90 min and 180 min post injection. Finally, in Paper V, the %ID/g of ^{125}I -labeled pretargeting molecule in the blood of normal BALB/c mice was monitored with and without administration of a polylysine-based clearing agent. Six mice were administered systemically with the iodinated pretargeting molecule. Three of them were given a clearing agent 23 h post injection of the pretargeting molecule, and 3 mice were not given any clearing agent. Serial blood samples were taken from the tail vein up to 46 h after injection of the ^{125}I -labeled pretargeting molecule. Radioactivity uptake in liver, kidney and blood was also evaluated 68 h post injection.

5 RESULTS

5.1 In vitro results of the immunoconjugates for ^{213}Bi - and ^{211}At -labeling (Papers I-III)

5.1.1 Structure analysis

In all FPLC analyses, results showed intact antibody structures after conjugation and labeling. For evaluation of the amount of chelators attached to the antibody for subsequent ^{213}Bi -labeling, an arsenazo III assay was performed, in which results exhibited 2 available chelators per antibody. The TNBS analysis, which was used to evaluate the average number of *m*-MeATE on the antibody, revealed 7 ATE linkers attached per antibody, while the ICP-MS revealed 6 MSB linkers per antibody.

5.1.2 Radiochemical purity

The radiochemical purity of the ^{213}Bi -labeled immunoconjugates was approximately 90-95%, as analyzed by ITLC. The radiochemical purity of both types of ^{211}At -labeled immunoconjugates was typically > 95%, as evaluated by methanol precipitation.

5.1.3 Cell binding

The immunoreactivity (B/T) of the ^{213}Bi -labeled antibodies was typically 70-85%, while the immunoreactivity of the ^{211}At -labeled antibodies was approximately 70-95%. Cell binding curves for the ^{213}Bi - and the ^{211}At -labeled antibodies are shown in Figure 10 and Figure 11. As seen in the figures, the cell binding occurs with a slower rate with the ^{213}Bi -labeled antibodies. This may be due to lower specific activity of the ^{213}Bi -immunoconjugates.

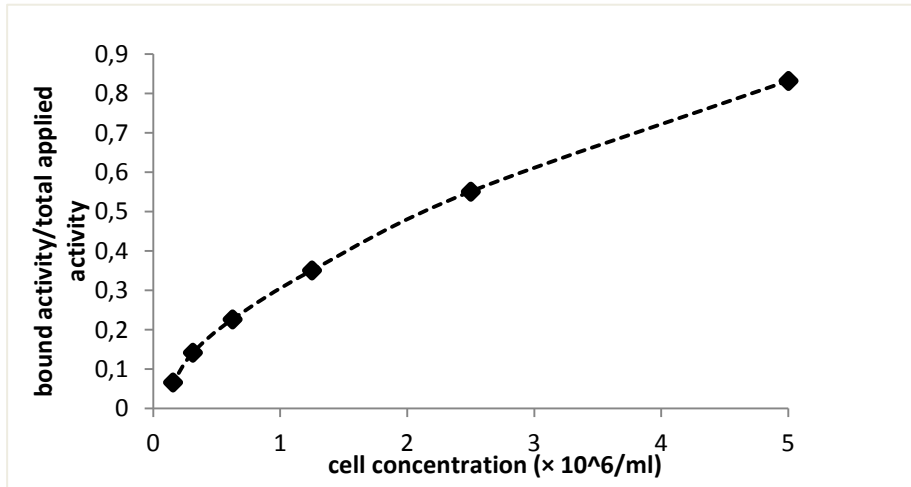


Figure 10. Binding of ^{213}Bi -MX35 to OVCAR-3 cells in suspensions of cell concentrations up to 5×10^6 cells/ml.

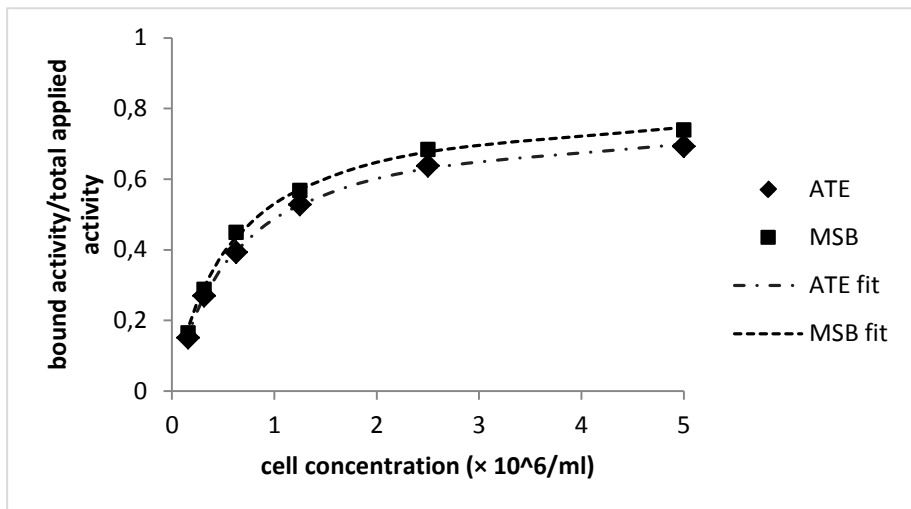


Figure 11. Binding of ^{211}At -MSB-MX35 and ^{211}At -ATE-MX35 to OVCAR-3 cells in suspensions of cell concentrations up to 5×10^6 cells/ml.

5.2 In vivo results for the ^{213}Bi - and ^{211}At -labeled immunoconjugates (Papers I-III)

5.2.1 Therapeutic efficacy and toxicity

In Paper I, the groups treated with ^{213}Bi -MX35 and ^{211}At -MX35 2 weeks after cell inoculation had tumor-free fractions (TFFs) of 0.60 and 0.90, respectively. The TFF in the control group was 0.20, i.e. clearly lower than in the treated groups. Although the group treated with ^{211}At -MX35 had a higher TFF, the difference between the treatment with ^{211}At -MX35 and ^{213}Bi -MX35 was not significant according to Fisher's exact test ($P = 0.065$). However, in the groups treated with ^{213}Bi -MX35 and ^{211}At -MX35 4 weeks after cell inoculation, the TFFs were only 0.25 in both groups, while the reference group had a TFF of 0. This means that there was no statistically significant difference between the treated groups and the untreated group. In Paper II, all mice were treated with ^{213}Bi -MX35 2 weeks after cell inoculation. The TFFs of the groups treated with 3 MBq and 9 MBq of ^{213}Bi -MX35 were 0.55 and 0.78, respectively, while the TFF of the control group receiving unlabeled MX35 was 0.15. According to Fisher's exact test, there was a statistical significance between the 9 MBq group and the reference group ($P = 0.0002$). The difference in TFF between the 3 MBq group and the reference group was borderline ($P = 0.0187$), because the significance level of 0.05 needs to be compensated for the multiple testing, and this is done by using the significance level $0.05/3 = 0.0167$ for each of the three pairwise tests. There was no statistical significance between the two treated groups ($P = 0.1818$). However, a Cochran-Armitage trend test indicated that there was a correlation between administered activity and TFF ($P = 0.0001$), implying that higher activity most likely increases TFF. The toxicity studies in Paper I and II did not reveal any significant toxicity for any of the treatments. The therapeutic efficacies in the two studies are summarized in Table 1 and Table 2. Examples of visualizations of macroscopic and microscopic tumors by H&E staining and IHC are shown in Figure 12.

Table 1. Results from the therapeutic efficacy study described in Paper I. Tumor incidence in the mouse groups treated with $^{213}\text{Bi-MX35}$, $^{211}\text{At-MX35}$, and the reference groups receiving no treatment. Group 5 was sacrificed together with groups 1 and 2, and group 6 was sacrificed together with groups 3 and 4.

Group	Treatment	Activity (MBq)	Macroscopic tumor (no. of animals)	Microscopic tumor (no. of animals)	Ascites (no. of animals)	TFF
1	$^{211}\text{At-MX35}$ 2 weeks after cell inoculation	0.4-0.5	2/20	0/20	0/20	0.90
2	$^{213}\text{Bi-MX35}$ 2 weeks after cell inoculation	3	6/20	2/20	0/20	0.60
3	$^{211}\text{At-MX35}$ 4 weeks after cell inoculation	0.4	15/20	0/20	4/20	0.25
4	$^{213}\text{Bi-MX35}$ 4 weeks after cell inoculation	3	15/20	0/20	3/20	0.25
5	Ref. group 1 (no treatment)	-	8/10	0/10	4/10	0.20
6	Ref. group 2 (no treatment)	-	10/10	0/10	5/10	0

TFF = tumor-free fraction, i.e. the fraction of mice with no macroscopic or microscopic tumors and no ascites. Microscopic tumors were only sought in mice with no macroscopic tumors and/or ascites; thus, "microscopic tumor" refers here to microscopic tumors without macroscopic tumor or ascites.

Table 2. Results from the therapeutic efficacy study described in Paper II. Tumor incidence in the two mouse groups treated with $^{213}\text{Bi-MX35}$ and in the reference group receiving unlabeled MX35. The treatments were given 2 weeks after cell inoculation.

Group	Treatment	Activity (MBq)	Macroscopic tumor (no. of animals)	Microscopic tumor (no. of animals)	Ascites (no. of animals)	TFF
1	$^{213}\text{Bi-MX35}$	3	4/20	9/20	0	0.55
2	$^{213}\text{Bi-MX35}$	9	1/18*	4/18*	0	0.78
3	Ref. group (cold MX35)	-	7/20	17/20	4	0.15

TFF = tumor-free fraction, i.e. the fraction of the mice with no macroscopic or microscopic tumors and no ascites. Microscopic tumors were sought in all mice, also in the animals with detected macroscopic tumors and/or ascites. * = two animals were excluded from the mouse group receiving 9 MBq; one was sacrificed earlier due to atypical mouse behavior (no tumor tissue could be detected), and one was excluded from the study due to a sole subcutaneous tumor outside of the peritoneum which was suspected to be the result of cell leakage from the peritoneal cavity post inoculation.

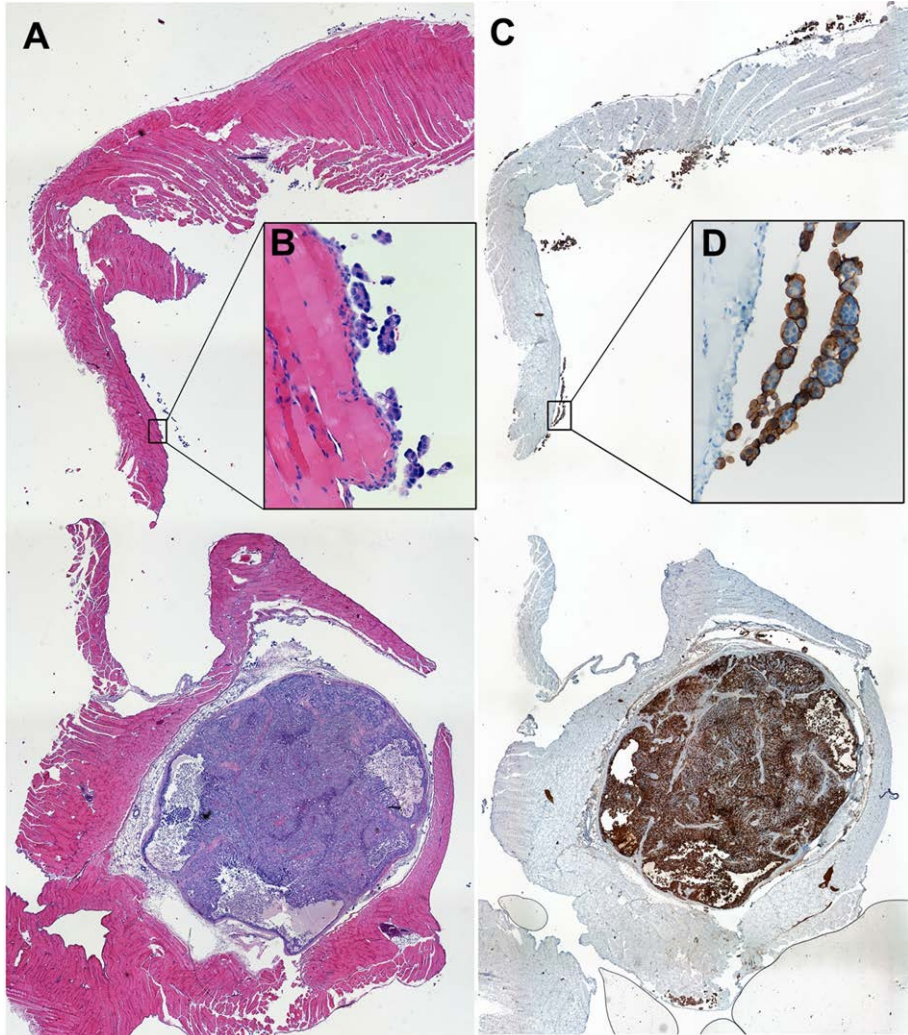


Figure 12. Tissue sections of the abdominal wall from a reference animal treated with unlabeled MX35 visualizing a macroscopic tumor (bottom of A and C) and microscopic tumors (B and D). A and B are stained with H&E while C and D show the dense distribution (in brown) of the MX35-antigen on tumor cells using IHC.

5.2.2 Biodistribution

The biodistribution study in Paper I was performed with intraperitoneally injected ^{213}Bi -MX35 and ^{211}At -MX35. The distributions of the two radioimmunoconjugates were monitored up to 180 min post injection, i.e. when up to 94 % of the ^{213}Bi had decayed. Longer timeframes post injection for ^{211}At -MX35 have already been considered in another study [122] and this was therefore not examined in this

study. The experiments showed a very similar biodistribution for ^{213}Bi -MX35 and ^{211}At -MX35, see Figure 13. This indicates that both radioimmunoconjugates had high radiochemical purity at the time of injection and that the molecules stayed intact to a high extent throughout the study. Otherwise, free ^{213}Bi would have accumulated in the kidneys and free ^{211}At would have accumulated in the thyroid. The study in Paper III compared the biodistribution between two ^{211}At -labeled immunoconjugates, with different linkers between the antibody and the astatine. The results showed a similar in vivo distribution for the ^{211}At -MSB-MX35 and ^{211}At -ATE-MX35 (Figure 14), without any significantly different activity uptakes in the selected organs, except for at the last time point (25 h; Figure 15). At 25 h, differences in blood, lung, kidney, muscle, heart and tumor could be seen, with lower uptakes for ^{211}At -MSB-MX35 in all tissues. However, the tumor-to-blood ratio was higher for ^{211}At -MSB-MX35 than for ^{211}At -ATE-MX35.

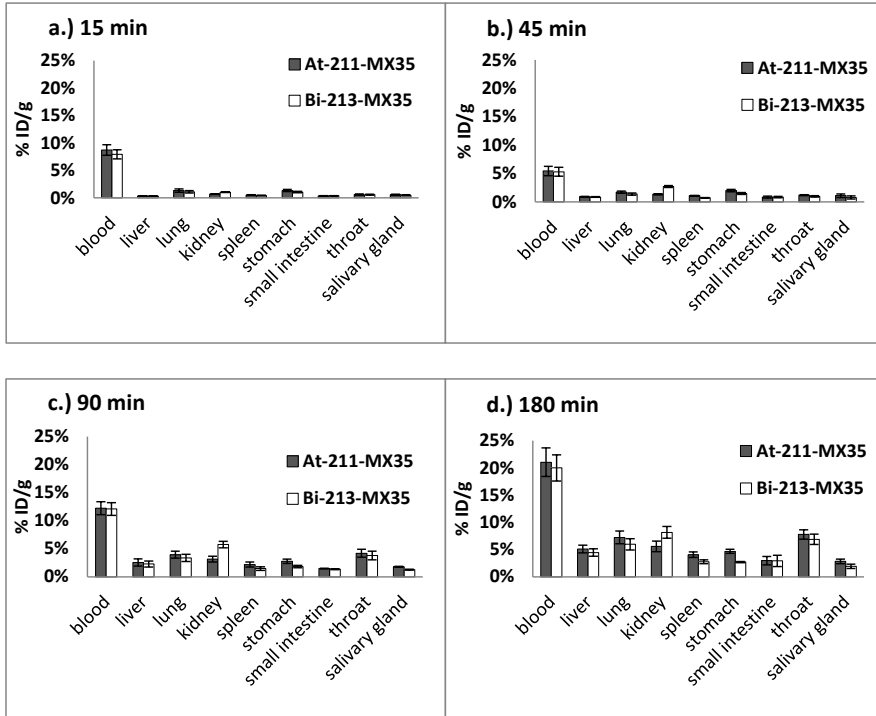


Figure 13. Biodistribution of intraperitoneally injected ^{211}At - and ^{213}Bi -labeled monoclonal antibody MX35. Mice were injected with a mixture of ^{211}At -MX35 and ^{213}Bi -MX35, and data were collected 15 min (a), 45 min (b), 90 min (c) and 180 min (d) post injection. Four animals were sacrificed at each time point. Tissue concentrations of radioactivity are expressed as the percentages of injected dose per gram (% ID/g). Means and SEM (error bars) are depicted.

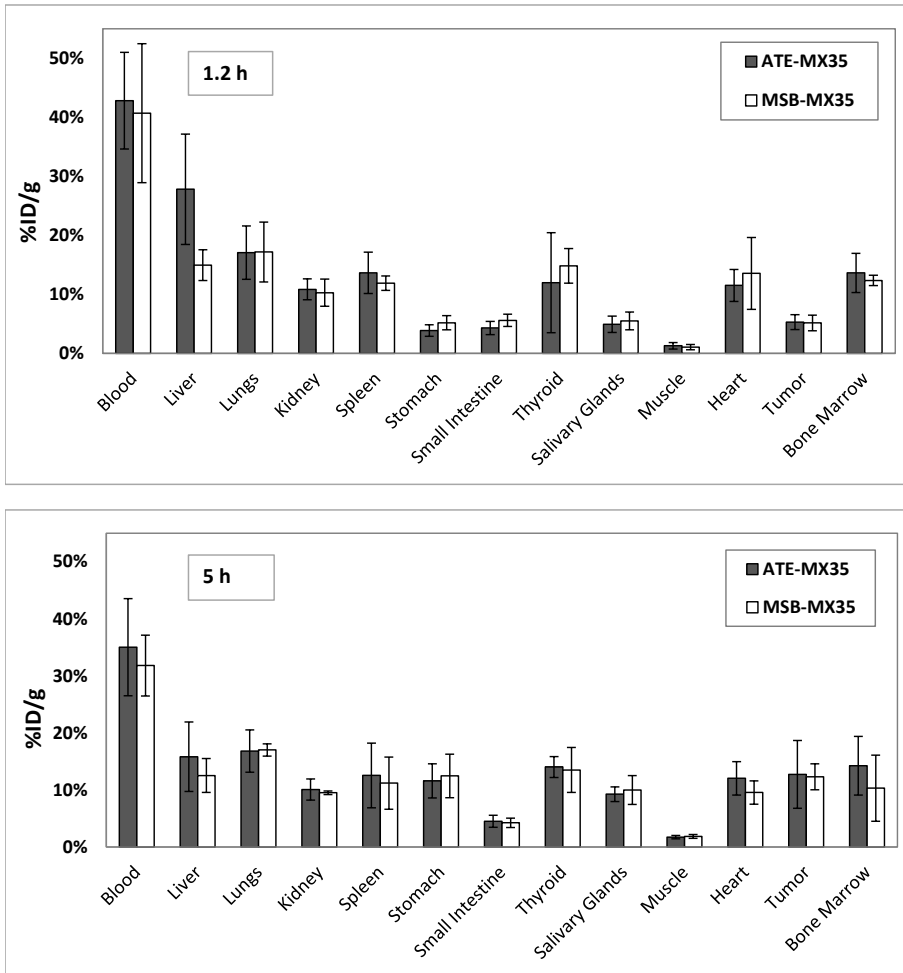


Figure 14. Biodistribution of systemically injected ^{211}At -labeled monoclonal antibody MX35 conjugated with ATE or MSB. Data were collected 1.2 h and 5 h post injection. Four animals per group were sacrificed at each time point. Tissue concentrations of radioactivity are expressed as the percentages of injected dose per gram (% ID/g).

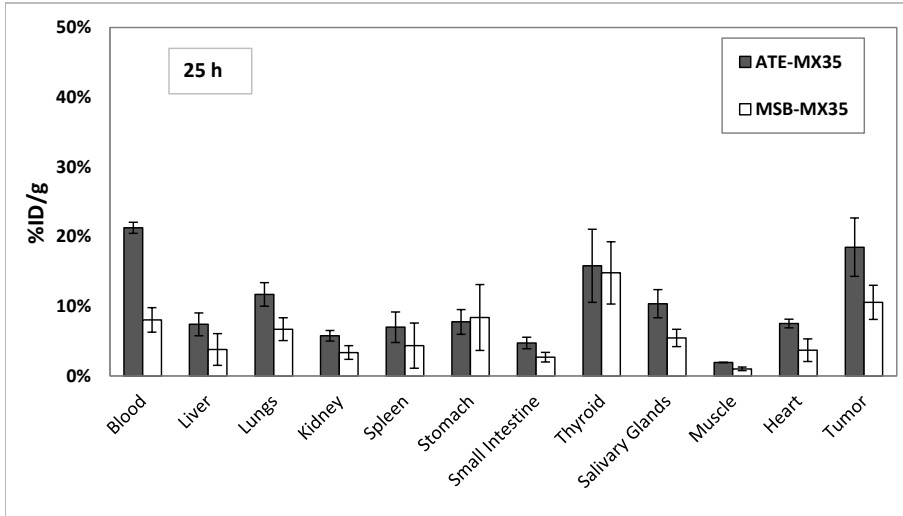


Figure 15. Biodistribution of systemically injected ^{211}At -labeled monoclonal antibody MX35 conjugated with ATE or MSB. Data were collected 25 h post injection, and each group contained four animals. Tissue concentrations of radioactivity are expressed as the percentages of injected dose per gram (% ID/g).

5.3 In vitro and in vivo results of the polylysine-based effector for pretargeted radioimmunotherapy and -imaging (Paper IV)

5.3.1 Structure analysis

Similar to the synthesis of the antibody conjugates produced for direct labeling, the synthesis of the polylysine-based effector molecule does not result in one defined molecule. Instead, it results in a range of different amounts of functional agents attached to the polylysine. The analyses performed showed that when adding a 5 fold molar excess of NHS-LC-biotin to the polylysine, 4 biotins on average were attached to the polymer after the reaction. After the reaction of the biotinylated polylysine with a 5, 10 or 15 fold molar excess of chelator, 5, 9 and 13 chelators were bound to the polylysine. No free amino groups could be detected by the TNBS analysis after charge-modification by succinylation of the remaining amines.

5.3.2 Radiochemical purity and avidin binding

The synthesized effectors were labeled with ^{213}Bi , ^{68}Ga and ^{111}In , and the radiolabeled purity after labeling was $> 97\%$, as evaluated by ITLC. The avidin binding was $> 92\%$.

5.3.3 Renal uptake study

The renal uptake of radioactivity was measured for effectors of two different sizes, based on poly-L-lysine of 30 and 50 lysine residues, respectively. Both polymers were reacted with a 5 fold molar excess of NHS-LC-biotin and a 10 fold molar excess of chelator, followed by charge-modification by succinylation. The total molecular weights of the effectors were 14 kDa and 19 kDa, respectively. The renal uptake study showed a significant difference in the uptake related to the different sizes of the molecules, see Figure 16. The molecule of larger size, and thus more negative net charge, had an average kidney uptake of approximately 1/4, compared with the smaller-sized molecule. The area under the curve (AUC) of the time-activity curves (TAC; i.e. the non-decay-corrected $\%$ ID/g values) was calculated for the ^{213}Bi -labeled effectors, as an estimation of the absorbed dose to the kidneys.

According to the AUCs, the absorbed dose to the kidneys was approximately 5 times lower for the 19 kDa effector.

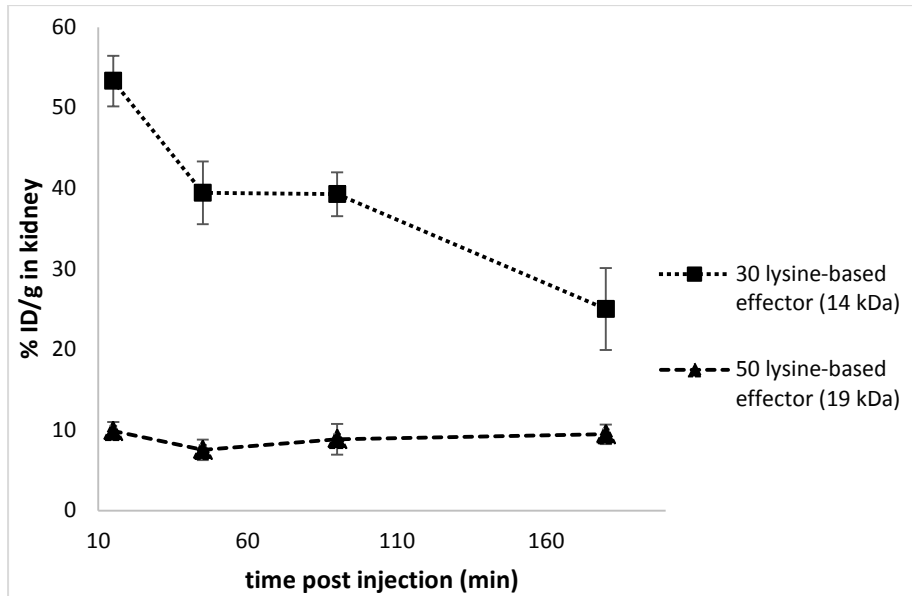


Figure 16. Radioactivity uptake in the kidney of effectors of two different sizes (14 kDa and 19 kDa). $n = 3$ for each time point. Means and standard error of the mean (SEM; error bars) are depicted.

5.4 In vivo results of the polylysine-based clearing agent for pretargeted radioimmunotherapy and -imaging (Paper V)

The ability to clear the blood of unbound pretargeting molecules was evaluated in vivo for the polylysine-based clearing agent. The results showed a significant decrease of pretargeting molecule concentration in the blood after injection of the polylysine-based clearing agent (Figure 17), indicating good clearing abilities. The kidney and liver uptakes of pretargeting molecule measured 68 h post injection showed elevated uptakes in both liver and kidney in the animals injected with the clearing agent (Figure 18).

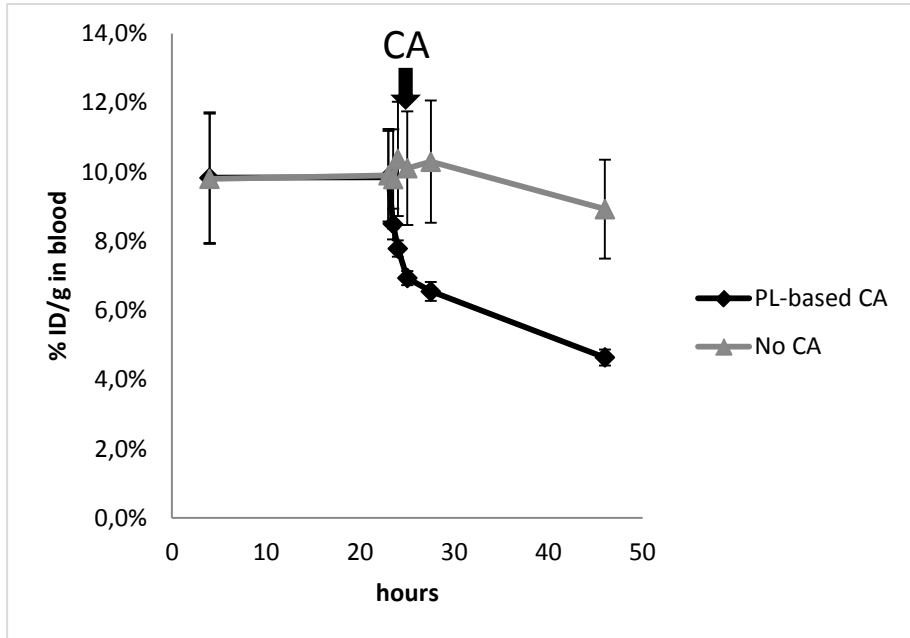


Figure 17. Effects of a poly-L-lysine-based clearing agent on circulating pretargeting molecules. Six BALB/c mice were injected i.v. with 1.4 nmol of ^{125}I -labeled pretargeting molecule at time 0. Three of the mice were injected i.v. 23 hours later with 5.8 nmol of clearing agent, whereas the other 3 mice did not receive any clearing agent. Serial blood samples were taken from the tail vein 4 h, 23 h, 23.5 h, 24 h, 25 h, 27.5 h and 46 h after the administration of the pretargeting molecule and analyzed in a γ counter. Means and SEM (error bars) are depicted.

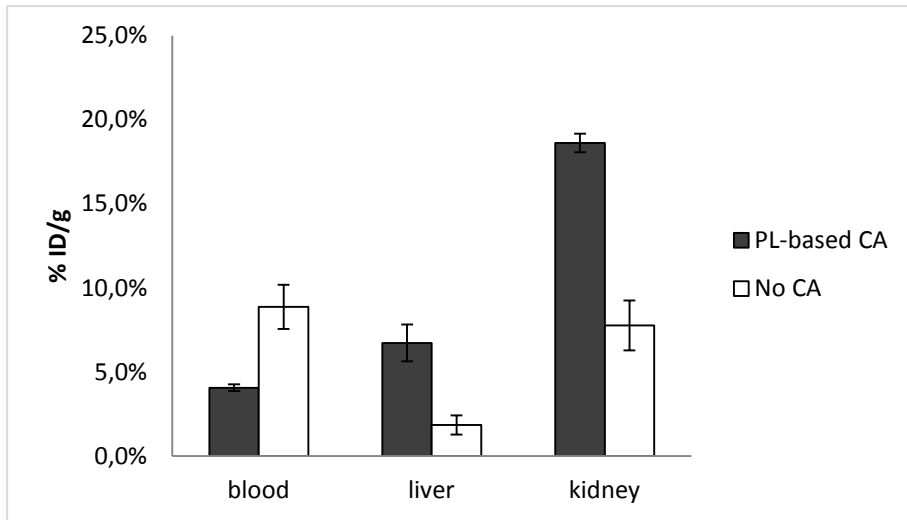


Figure 18. Organ uptakes of ^{125}I -labeled pretargeting molecule (or fragments thereof) 68 h after administration in mice receiving polylysine-based clearing agent compared with reference animals not receiving any clearing agent. Means and SEM (error bars) are depicted.

6 DISCUSSION

6.1 General

It is generally not primary tumors, but metastases, that are responsible for most cancer deaths [1]. Malignant cells are able to detach from the original tumor and disseminate to other organs distant from the original tumor site, enabling metastatic growth in various organs. Targeted cancer therapies like RIT have been developed to reach tumor cells in the body not reachable by other means. The principle of RIT, i.e. a targeting vector (the tumor-specific antibody) attached to a cytotoxic entity (the radionuclide), is promising for metastatic cancer treatment, particularly for micrometastases in an adjuvant setting. However, current techniques are often limited by narrow therapeutic windows, i.e. low tumor dose as compared to normal tissue dose. Radiation-induced cell death occurs preferentially in proliferating cells, which is advantageous in cancer treatment since malignant cell populations often proliferate to a high degree. However, there are also normal tissues with a high dividing rate, e.g. the bone marrow and the mucosal lining of the gastrointestinal tract, resulting in radiation sensitivity and thus limiting the possible dose that can be given to the patient. This is particularly problematic when the therapeutic agent is given systemically, but may be less of an issue for intracavitary treatment, for example the intraperitoneal treatment of ovarian cancer. In cases where the treatment has to be administered systemically, an approach other than conventional RIT may have to be used, since the pharmacokinetics of radiolabeled antibodies is unfavorable (the slow distribution of antibodies leads to irradiation of sensitive normal tissues). Therefore, pretargeting approaches are in general preferable for systemic treatments.

This PhD project has focused on the development of conventional RIT for intracavitary therapy, as well as pretargeted RIT (PRIT) for future systemic treatments. Since micrometastases have been the main focus of the treatments, the radionuclides chosen for therapeutic use have been the α emitters ^{213}Bi and ^{211}At . These radionuclides have suitable properties and half-lives, allowing time both for radiolabeling the vector

and for distribution within the organism. Furthermore, they disintegrate without long-lived α -emitting daughter nuclides in their decay chain, limiting the risk of α -emitting nuclides escaping far from the targeted cells. The first three papers included in this thesis have focused on biodistribution and/or the therapeutic efficacy of conventional α -RIT, whereas in the last two papers, molecules for future pretargeted treatments were developed and evaluated.

6.1.1 *Papers I-II*

In the first two papers, the therapeutic efficacy of α -RIT was evaluated in an ovarian cancer mouse model. In general, α -RIT was effective in the treatment of microscopic ovarian cancer tumors. A weakness in the evaluation of tumor presence was that it was not experimentally possible to examine the whole peritoneum/abdominal wall and mesentery of each mouse with microscopy. It is apparent that only an extremely small sample of the peritoneal lining can be scrutinized and microscopically examined. Therefore, only a limited number of sections from the biopsies of the peritoneum were chosen to represent the intraperitoneal cavity as a whole. The examination undertaken in the study of the second paper was more extensive than in that of the first paper. In the first paper, the mesentery as well as a quadratic section of the parietal peritoneum from the abdominal wall was examined by microscopy, but only in cases where no macroscopic tumors or ascites were detected. In the second paper, the examination approach was extended. As tumor deposits often occurred on the surface of the spleen after intraperitoneal inoculation of OVCAR-3 cells, the spleen of each mouse was also examined. Additionally, the tissues of all mice included in the study were examined by microscopy, even in cases where macroscopic tumors and/or ascites had already been detected.

Other analyses could be added to the examination performed to potentially enhance the accuracy of tumor incidence recorded in the mice. One example is evaluation of the presence of carcinoma antigen 125 (CA-125) in the mouse blood serum. The CA-125 concentration in the serum of OVCAR-3 tumor xenografts has been shown to correlate well with disease progression and could predict at an early stage the efficacy of the treatment [123]. Another method to facilitate tumor

detection at the time of dissection would be to use green fluorescent protein (GFP) transfected cells and investigate tumor presence using fluorescence microscopy. Yet another strategy, which could potentially also be used for tumor detection in patients with peritoneal carcinosis, is to perform peritoneal lavage with 5-aminolevulinic acid (ALA) [124]. ALA accumulates in the tumors and metabolizes to protoporphyrin IX, which is a fluorescent agent [125]. This type of laparoscopic fluorescence diagnosis has been shown to detect 35% additional tumor foci in rats compared to laparoscopy with white-light alone [124]. Using fluorescently labeled tumor-specific antibodies for laparoscopic diagnosis has produced good results in other tumor models [126, 127], and could potentially also be used in our ovarian cancer model, as well as in ovarian cancer patients.

One general aspect to consider in therapeutic efficacy experiments in the ovarian cancer mouse model is that the model may not behave in the same way as the clinical reality. The xenograft tumors grow for 2-4 weeks in the immunodeficient mice and may therefore have a different tumor growth pattern than in humans, who most often have had tumor growth for a significantly longer period of time at the point of diagnosis. The relevance of using the intraperitoneal treatment approach is based on the clinical finding that most relapses post-surgery and post systemic chemotherapy occur intraabdominally. It is well known that retroperitoneal lymph nodes are frequently invaded, but they are most likely eliminated by intravenous chemotherapy due to the presence of vasculature. In contrast, intraabdominal deposits primarily lack blood vessels and therefore elude the systemic chemotherapy.

6.1.2 Paper III

In the third paper, the synthesized *N*-[2-(maleimido)ethyl]-3-(trimethylstannyl)benzamide (MSB) was evaluated as a coupling agent for ²¹¹At-labeling of antibodies for prospective use in therapeutic efficacy studies with α -RIT. A biodistribution study was performed to evaluate whether the recently developed MSB reagent was advantageous as a coupling agent in comparison with the commercially available *m*-MeATE. The advantage of using MSB is that the molecule is site-selective, because it primarily reacts with the available cysteine-cysteine bridges situated

in the hinge region of the antibody [128], while the lysine-reactive *m*-MeATE binds more randomly to the antibody. This can result in *m*-MeATE-binding at the antigen-binding site, causing reduced immunoreactivity. Another advantage of having a site-selective coupling agent is that the biodistribution of the conjugates may be more uniform due to less variation in the molecular structure. The results of the *in vivo* distribution study showed very similar biodistribution for the MSB-and the ATE-conjugates. However, 25 h post injection, a difference could be seen. Several tissues had a lower activity uptake in the animals receiving the MSB-conjugates. However, the tumor-to blood ratio was higher for the MSB-conjugates at this point in time compared with the ATE-conjugates. The difference in tissue uptakes could be caused by loss of fragments of the MSB-conjugated antibody due to the already present modifications of the disulfide bridges. This would lead to a faster blood clearance for the MSB-conjugates. If this is the case, radiolabeled fragments containing the antigen-binding site, i.e. F(ab)₂ or F(ab) fragments, should remain to a high extent since the tumor uptake remained high. Antibody fragmentation due to reactions in the hinge region could be caused by reactive oxygen species *in vivo* [129]. However, since antibody conjugation with MSB resulted in a higher tumor-to blood ratio than conjugation with ATE, the MSB coupling reagent is a viable alternative to commercially available ATE.

6.1.3 *Papers IV-V*

In the last two papers, molecules for PRIT were synthesized and evaluated. In Paper IV, polylysine-based effectors of two different sizes were produced, radiolabeled and evaluated. The *in vitro* evaluation exhibited promising results, and the renal uptake was shown to be altered to a great extent by modifying the molecule's size and charge. In Paper V, a polylysine-based clearing agent was synthesized to accelerate blood clearance of unbound pretargeting molecules. The *in vivo* study showed a rapid decrease in blood concentration of the pretargeting molecule, exhibiting promise for further studies of polylysine-based clearing agents.

However, the polylysine-based molecules have not yet shown their functionality in full pretargeting systems. A preliminary biodistribution

study was performed with the polylysine-based effector, where the tumor uptake unfortunately was inconclusive. This was most probably due to problems in the pretargeting molecule (antibody-streptavidin) production; however, in vivo dissociation of the synthesized effector cannot be completely excluded. The polylysine-based clearing agent has high potential to work in a full pretargeting system; however, there are other clearing agents, e.g. the *N*-acetyl galactosamine- and biotin-containing NAGB which exhibit a faster and more extensive blood clearing of antibody-streptavidin molecules [130]. Nevertheless, the polylysine-based clearing agent can be rapidly modified for optimization of the clearing function. Another question arising concerning the polylysine-based clearing agent is what the consequences are of the elevated uptake of pretargeting molecule in the liver and kidney after clearing agent administration. If the pretargeting molecules in the liver and kidney are still intact, this may lead to elevated uptakes of effector molecule, resulting in elevated absorbed dose to those tissues.

The pretargeting agents in this PhD project were synthesized using streptavidin and biotin for high affinity between the pretargeting molecule and the effector. Although the (strept)avidin-biotin system has many advantages, it also has some shortcomings, for example that endogenous biotin may disrupt a patient treatment with PRIT. Another disadvantage is the likely immune response to injected streptavidin, which may hinder multiple treatments. There are strategies to deal with endogenous biotin as well as the immunogenicity of (strept)avidin such as changing the (strept)avidin structure to lower the immune response [131-134] and to decrease the affinity for endogenous biotin [135-137]. However, an even better way to deal with the complications posed by biotin and streptavidin may be to substitute them with other molecules. Many papers have been published over the last few years examining the possibility of using click chemistry with *trans*-cyclooctene (TCO) and tetrazine for example for pretargeting in therapy and imaging [45-47]. As these molecules do not appear to interact with endogenous molecules but maintain a very high affinity for each other, their use may be a point of future success within pretargeting.

7 CONCLUSIONS AND FUTURE PERSPECTIVES

This PhD project has resulted in numerous *in vitro* evaluations and several *in vivo* evaluations of molecules for RIT and PRIT. The evaluation of ^{213}Bi -labeled MX35 in an ovarian cancer mouse model has never been undertaken before. Positive therapeutic efficacy and toxicity results were obtained from the studies, which encourage further preclinical experiments. Therapeutic efficacy with different activity levels of ^{213}Bi -MX35 should be explored further, as well as different specific activities of the radioimmunoconjugate. Clinical studies of ^{213}Bi -labeled mAbs in ovarian cancer patients would also be a very interesting and worthwhile undertaking, to be compared with the clinical trials with ^{211}At . The site-specific MSB for astatination of antibodies was shown to be an interesting alternative to the commercially available ATE-linker, and should be studied further, for example in preclinical evaluations of therapeutic efficacy.

In the development of effector molecules for pretargeting, some interesting findings were made. As previously stated, the polylysine framework provides many possibilities for variation in the molecular size and charge. A hypothesis was that a slightly larger polylysine base would result in more favorable clearance, resulting from the more negative net charge after succinylation. The reason is that more negatively charged molecules are more restricted from renal filtration [138]. This was indeed the case in our renal uptake study comparing effectors built on a polylysine scaffold of 30 and 50 lysine residues, respectively. In future biodistribution studies of polylysine-based molecules, more organs should be studied, as well as additional sizes of the polylysine base, for determination of the overall optimum biodistribution. Another possibility outside of using polylysine in the synthesis of the effectors could be for example to use polycysteine for coupling maleimido derivatives of biotin and chelators. A polycysteine base could possibly result in an more favorable biodistribution. Another aspect of the polylysine-based effectors which should be studied in the near future is their functionality in a complete pretargeting system. If

they do not properly target the tumor cells, or do not stay intact on the cells, modifications in the molecular structure would be needed.

The polylysine-based clearing agent exhibited a promising clearing function, and should be optimized with respect to size, charge and amount of functional groups attached. The synthesized clearing agent should also be studied in a complete pretargeting system, to investigate whether the elevated uptakes of the pretargeting molecules in the liver and kidney also result in elevated uptakes of radioactivity in these organs. If this were to occur, modifications in the structure of the clearing agent would be crucial.

When the pretargeting system has demonstrated satisfying tumor targeting capacity *in vivo*, it would be very interesting to investigate and evaluate the biodistribution and therapeutic efficacy for α -PRIT. Since pretargeting provides much better prospects for systemic treatments with short-lived radionuclides, treatment of other cancer forms in addition to ovarian cancer would be feasible. It may also be possible to treat somewhat larger tumors with α -PRIT, but possibly not with conventional α -RIT. Uniform intra-tumoral distributions has proven to be possible in times as short as 30-45 min post injection for PRIT [139, 140], which does not appear to be achievable through conventional RIT [140].

An important aspect when working with α emitters is small scale dosimetry. Because of the short path length of α particles, non-uniformity of the activity distribution results in a non-uniform dose distribution. Thus, although transversal of 1-5 α particles to a cell gives a high probability of cell death, an average of 1-5 α particles emissions per cell in a tumor may also result in many cells staying alive if the radioactivity is unevenly distributed. Therefore, the uniformity in the tumor distribution of the targeting vectors will also be taken under consideration more and more in targeted α therapy. Small scale dosimetry for normal tissue is of course equally important to be able to determine the therapeutic window. Small-scale imaging systems, i.e. the α camera [141], are likely to be important tools for improved dosimetry of α emitters.

Technological advances in molecular engineering have broadened the supply of targeting agents for RIT [142, 143]. There are now multiple forms of targeting vectors that can enhance pharmacokinetics and targeting properties for each desired field of application. Together with pretargeting, molecular engineering will most likely be an important factor in the future development of targeted therapy.

8 ACKNOWLEDGEMENTS

First of all, I would like to thank my supervisor **Sture Lindegren**. You gave me this job to begin with, and for that I am most grateful. Without your ideas and enthusiasm, this PhD project would not have existed in the first instance.

I would also like to thank my very engaged assistant supervisor **Tom Bäck**. You spent a lot of time with me in the office as well as at EBM, and it has been fun to discuss everything from the α camera and physiology to psychology and literature with you.

I would like to thank my other assistant supervisor as well, our Head of Group **Per Albertsson**. We have had very interesting conversations about oncology, and I would add a special thank you for the interesting round tour in the external radiation therapy facilities.

Additionally, I would like to send a special thank you to my former assistant supervisor **Lars Jacobsson**. I am very grateful for your theoretical and emotional support, and I hope I can one day return at least something of everything you have given to me.

A special thank you also to **Ragnar Hultborn**, who spent this Christmas analyzing approximately one thousand tissue samples by microscopy for the final ^{213}Bi study. You also spent many hours discussing research and other things with me although you were not formally my supervisor. I am truly impressed by your never-ending engagement in medical research.

I also thank other present and former members of the targeted alpha therapy group: **Emma Aneheim** for being a good lab and discussion partner, **Helena Kahu** for culturing cells and for spending hours with me at EBM, **Elin Cederkrantz**, **Sofia Frost**, **Stig Palm**, **Jörgen Elgqvist**, **Kecke Elmroth**, **Ulla Delle**, **Karin Magnander**, **Mia Johansson**, **Andreas Hallqvist**, **Håkan Andersson**, **Nicolas Chouin** and **Holger Jensen**.

I would also like to thank my present and former fellow PhD students at Radiofysik, especially **Jenny Nilsson**, **Viktor Sandblom**, **Johan Spetz**, **Britta Langen**, **Joel Larsson**, **Emma Hedin**, **Ingun Ståhl**, **Christina Söderman**, **Anders Josefsson**, **Nils Rudqvist**, **Rimon Thomas**, **Arman**

Romiani, Malin Larsson, Alexa von Wrangel, Jonny Hansson, Mikael Montelius, Maria Larsson, Johanna Dalmo, Tobias Magnander, Jens Hemmingsson and Linn Hagmarker.

I would like to thank my other colleagues at Radiofysik as well, especially **Gunilla Adielson** who has done a lot of work for us in maintenance and support. I would also like to thank our Head of Department **Eva Forssell-Aronsson** for her support when I have needed it.

I also thank my parents, my mother **Lisbeth Sundberg** and her husband **Lennart Sundberg**, my father **Staffan Gustafsson** and his wife **Eivor Gustafsson**. I would also like to thank my brothers and my sister.

I would like to thank my daughter **Freja Gustafsson Lutz**, who is the joy of my life, and my husband **Georg Lutz**, who has put up with me through good and bad for the last twelve years.

Thank you.

9 REFERENCES

1. Chambers, A.F., A.C. Groom, and I.C. MacDonald, *Dissemination and growth of cancer cells in metastatic sites*. Nat Rev Cancer, 2002. **2**(8): p. 563-72.
2. Pantel, K., R.J. Cote, and O. Fodstad, *Detection and clinical importance of micrometastatic disease*. J Natl Cancer Inst, 1999. **91**(13): p. 1113-24.
3. Pantel, K. and G. Riethmuller, *Micrometastasis detection and treatment with monoclonal antibodies*. Curr Top Microbiol Immunol, 1996. **213 (Pt 3)**: p. 1-18.
4. Strebhardt, K. and A. Ullrich, *Paul Ehrlich's magic bullet concept: 100 years of progress*. Nat Rev Cancer, 2008. **8**(6): p. 473-80.
5. Pressman, D. and L. Korngold, *The in vivo localization of anti-Wagner-osteogenic-sarcoma antibodies*. Cancer, 1953. **6**(3): p. 619-23.
6. Barker, P.A., et al., *A study of the preparation, localization, and effects of antitumor antibodies labeled with I131*. Cancer Res, 1956. **16**(8): p. 761-73.
7. Goldenberg, D.M., et al., *Use of radiolabeled antibodies to carcinoembryonic antigen for the detection and localization of diverse cancers by external photoscanning*. N Engl J Med, 1978. **298**(25): p. 1384-6.
8. Goldenberg, D.M., et al., *Experimental radioimmunotherapy of a xenografted human colonic tumor (GW-39) producing carcinoembryonic antigen*. Cancer Res, 1981. **41**(11 Pt 1): p. 4354-60.
9. Goldenberg, D.M., *Targeted therapy of cancer with radiolabeled antibodies*. J Nucl Med, 2002. **43**(5): p. 693-713.
10. Goldenberg, D.M., *Advancing role of radiolabeled antibodies in the therapy of cancer*. Cancer Immunol Immunother, 2003. **52**(5): p. 281-96.
11. Kirkwood, J.M., et al., *Immunotherapy of cancer in 2012*. CA Cancer J Clin, 2012. **62**(5): p. 309-35.
12. Newsome, B.W. and M.S. Ernstoff, *The clinical pharmacology of therapeutic monoclonal antibodies in the treatment of malignancy; have the magic bullets arrived?* Br J Clin Pharmacol, 2008. **66**(1): p. 6-19.
13. Larson, S.M., et al., *Radioimmunotherapy of human tumours*. Nat Rev Cancer, 2015. **15**(6): p. 347-60.
14. Boerman, O.C., et al., *Pretargeted radioimmunotherapy of cancer: progress step by step*. J Nucl Med, 2003. **44**(3): p. 400-11.

15. Goldenberg, D.M., et al., *Antibody pretargeting advances cancer radioimmunodetection and radioimmunotherapy*. J Clin Oncol, 2006. **24**(5): p. 823-34.
16. Reardan, D.T., et al., *Antibodies against metal chelates*. Nature, 1985. **316**(6025): p. 265-8.
17. Goodwin, D.A., et al., *Monoclonal antibodies as reversible equilibrium carriers of radiopharmaceuticals*. Int J Rad Appl Instrum B, 1986. **13**(4): p. 383-91.
18. Goodwin, D.A., et al., *Pre-targeted immunoscintigraphy of murine tumors with indium-111-labeled bifunctional haptens*. J Nucl Med, 1988. **29**(2): p. 226-34.
19. Reilly, R.M., *Radioimmunotherapy of solid tumors: the promise of pretargeting strategies using bispecific antibodies and radiolabeled haptens*. J Nucl Med, 2006. **47**(2): p. 196-9.
20. Sharkey, R.M., et al., *Bispecific antibody pretargeting of radionuclides for immuno single-photon emission computed tomography and immuno positron emission tomography molecular imaging: an update*. Clin Cancer Res, 2007. **13**(18 Pt 2): p. 5577s-5585s.
21. Lindegren, S. and S.H. Frost, *Pretargeted radioimmunotherapy with alpha-particle emitting radionuclides*. Curr Radiopharm, 2011. **4**(3): p. 248-60.
22. Sakahara, H. and T. Saga, *Avidin-biotin system for delivery of diagnostic agents*. Adv Drug Deliv Rev, 1999. **37**(1-3): p. 89-101.
23. Lesch, H.P., et al., *Avidin-biotin technology in targeted therapy*. Expert Opin Drug Deliv, 2010. **7**(5): p. 551-64.
24. Hnatowich, D.J., F. Virzi, and M. Rusckowski, *Investigations of avidin and biotin for imaging applications*. J Nucl Med, 1987. **28**(8): p. 1294-302.
25. Sung, C. and W.W. van Osdol, *Pharmacokinetic comparison of direct antibody targeting with pretargeting protocols based on streptavidin-biotin binding*. J Nucl Med, 1995. **36**(5): p. 867-76.
26. Le Doussal, J.M., et al., *In vitro and in vivo targeting of radiolabeled monovalent and divalent haptens with dual specificity monoclonal antibody conjugates: enhanced divalent hapten affinity for cell-bound antibody conjugate*. J Nucl Med, 1989. **30**(8): p. 1358-66.
27. Goodwin, D.A., et al., *Pretargeted immunoscintigraphy: effect of hapten valency on murine tumor uptake*. J Nucl Med, 1992. **33**(11): p. 2006-13.
28. Boerman, O.C., et al., *Pretargeting of renal cell carcinoma: Improved tumor targeting with a bivalent chelate*. Cancer Research, 1999. **59**(17): p. 4400-4405.
29. Le Doussal, J.M., et al., *Targeting of indium 111-labeled bivalent hapten to human melanoma mediated by bispecific monoclonal*

- antibody conjugates: imaging of tumors hosted in nude mice.* Cancer Res, 1990. **50**(11): p. 3445-52.
30. Gautherot, E., et al., *Delivery of therapeutic doses of radioiodine using bispecific antibody-targeted bivalent haptens.* J Nucl Med, 1998. **39**(11): p. 1937-43.
 31. Kraeber-Bodere, F., et al., *Toxicity and efficacy of radioimmunotherapy in carcinoembryonic antigen-producing medullary thyroid cancer xenograft: comparison of iodine 131-labeled F(ab')₂ and pretargeted bivalent hapten and evaluation of repeated injections.* Clin Cancer Res, 1999. **5**(10 Suppl): p. 3183s-3189s.
 32. Gautherot, E., et al., *Pretargeted radioimmunotherapy of human colorectal xenografts with bispecific antibody and 131I-labeled bivalent hapten.* J Nucl Med, 2000. **41**(3): p. 480-7.
 33. Khaw, B.A., Y. Tekabe, and L.L. Johnson, *Imaging experimental atherosclerotic lesions in ApoE knockout mice: enhanced targeting with Z2D3-anti-DTPA bispecific antibody and 99mTc-labeled negatively charged polymers.* J Nucl Med, 2006. **47**(5): p. 868-76.
 34. Gada, K.S., et al., *Pretargeted gamma imaging of murine metastatic melanoma lung lesions with bispecific antibody and radiolabeled polymer drug conjugates.* Nucl Med Commun, 2011. **32**(12): p. 1231-40.
 35. Khaw, B.A., et al., *Bispecific antibody complex pre-targeting and targeted delivery of polymer drug conjugates for imaging and therapy in dual human mammary cancer xenografts: targeted polymer drug conjugates for cancer diagnosis and therapy.* Eur J Nucl Med Mol Imaging, 2014. **41**(8): p. 1603-16.
 36. Wang, Y., et al., *Pretargeting with amplification using polymeric peptide nucleic acid.* Bioconjug Chem, 2001. **12**(5): p. 807-16.
 37. He, J., et al., *Amplification targeting: a modified pretargeting approach with potential for signal amplification-proof of a concept.* J Nucl Med, 2004. **45**(6): p. 1087-95.
 38. Kuijpers, W.H., et al., *Specific recognition of antibody-oligonucleotide conjugates by radiolabeled antisense nucleotides: a novel approach for two-step radioimmunotherapy of cancer.* Bioconjug Chem, 1993. **4**(1): p. 94-102.
 39. Mang'era, K.O., et al., *Initial investigations of 99mTc-labeled morpholinos for radiopharmaceutical applications.* Eur J Nucl Med, 2001. **28**(11): p. 1682-9.
 40. He, J., et al., *Affinity enhancement bivalent morpholino for pretargeting: initial evidence by surface plasmon resonance.* Bioconjug Chem, 2005. **16**(2): p. 338-45.
 41. He, J., et al., *Affinity enhancement bivalent morpholinos for pretargeting: surface plasmon resonance studies of molecular dimensions.* Bioconjug Chem, 2005. **16**(5): p. 1098-104.

42. Chmura, A.J., M.S. Orton, and C.F. Meares, *Antibodies with infinite affinity*. Proc Natl Acad Sci U S A, 2001. **98**(15): p. 8480-4.
43. Chmura, A.J., et al., *Electrophilic chelating agents for irreversible binding of metal chelates to engineered antibodies*. J Control Release, 2002. **78**(1-3): p. 249-58.
44. Corneillie, T.M., et al., *Converting weak binders into infinite binders*. Bioconjug Chem, 2004. **15**(6): p. 1389-91.
45. Zeng, D., et al., *The growing impact of bioorthogonal click chemistry on the development of radiopharmaceuticals*. J Nucl Med, 2013. **54**(6): p. 829-32.
46. Knight, J.C. and B. Cornelissen, *Bioorthogonal chemistry: implications for pretargeted nuclear (PET/SPECT) imaging and therapy*. Am J Nucl Med Mol Imaging, 2014. **4**(2): p. 96-113.
47. Reiner, T. and B.M. Zeglis, *The inverse electron demand Diels-Alder click reaction in radiochemistry*. J Labelled Comp Radiopharm, 2014. **57**(4): p. 285-90.
48. Kolb, H.C., M.G. Finn, and K.B. Sharpless, *Click Chemistry: Diverse Chemical Function from a Few Good Reactions*. Angew Chem Int Ed Engl, 2001. **40**(11): p. 2004-2021.
49. Debets, M.F., et al., *Bioconjugation with Strained Alkenes and Alkynes*. Accounts of Chemical Research, 2011. **44**(9): p. 805-815.
50. Sletten, E.M. and C.R. Bertozzi, *From Mechanism to Mouse: A Tale of Two Bioorthogonal Reactions*. Accounts of Chemical Research, 2011. **44**(9): p. 666-676.
51. Becer, C.R., R. Hoogenboom, and U.S. Schubert, *Click Chemistry beyond Metal-Catalyzed Cycloaddition*. Angewandte Chemie-International Edition, 2009. **48**(27): p. 4900-4908.
52. Jewett, J.C. and C.R. Bertozzi, *Cu-free click cycloaddition reactions in chemical biology*. Chemical Society Reviews, 2010. **39**(4): p. 1272-1279.
53. Knall, A.C. and C. Slugovc, *Inverse electron demand Diels-Alder (iEDDA)-initiated conjugation: a (high) potential click chemistry scheme*. Chemical Society Reviews, 2013. **42**(12): p. 5131-5142.
54. Schoch, J., et al., *Site-Specific One-Pot Dual Labeling of DNA by Orthogonal Cycloaddition Chemistry*. Bioconjugate Chemistry, 2012. **23**(7): p. 1382-1386.
55. Kohler, G. and C. Milstein, *Continuous cultures of fused cells secreting antibody of predefined specificity*. Nature, 1975. **256**(5517): p. 495-7.
56. Kricka, L.J., *Human anti-animal antibody interferences in immunological assays*. Clin Chem, 1999. **45**(7): p. 942-56.
57. Huhlov, A. and K.A. Chester, *Engineered single chain antibody fragments for radioimmunotherapy*. Q J Nucl Med Mol Imaging, 2004. **48**(4): p. 279-88.

58. Lofblom, J., et al., *Affibody molecules: engineered proteins for therapeutic, diagnostic and biotechnological applications*. FEBS Lett, 2010. **584**(12): p. 2670-80.
59. Boswell, C.A., et al., *Compartmental Tissue Distribution of Antibody Therapeutics: Experimental Approaches and Interpretations*. Aaps Journal, 2012. **14**(3): p. 612-618.
60. Rao, A.V., G. Akabani, and D.A. Rizzieri, *Radioimmunotherapy for Non-Hodgkin's Lymphoma*. Clin Med Res, 2005. **3**(3): p. 157-65.
61. Gopal, A.K., et al., *131I anti-CD45 radioimmunotherapy effectively targets and treats T-cell non-Hodgkin lymphoma*. Blood, 2009. **113**(23): p. 5905-10.
62. Chan, J.K., C.S. Ng, and P.K. Hui, *A simple guide to the terminology and application of leucocyte monoclonal antibodies*. Histopathology, 1988. **12**(5): p. 461-80.
63. Coliva, A., et al., *90Y Labeling of monoclonal antibody MOv18 and preclinical validation for radioimmunotherapy of human ovarian carcinomas*. Cancer Immunol Immunother, 2005. **54**(12): p. 1200-13.
64. Smith-Jones, P.M., et al., *Preclinical radioimmunotargeting of folate receptor alpha using the monoclonal antibody conjugate DOTA-MORAb-003*. Nucl Med Biol, 2008. **35**(3): p. 343-51.
65. Zacchetti, A., et al., *(177)Lu- labeled MOv18 as compared to (131)I- or (90)Y-labeled MOv18 has the better therapeutic effect in eradication of alpha folate receptor-expressing tumor xenografts*. Nucl Med Biol, 2009. **36**(7): p. 759-70.
66. Yin, B.W., et al., *Monoclonal antibody MX35 detects the membrane transporter NaPi2b (SLC34A2) in human carcinomas*. Cancer Immun, 2008. **8**: p. 3.
67. Gryshkova, V., et al., *The study of phosphate transporter NAPI2B expression in different histological types of epithelial ovarian cancer*. Exp Oncol, 2009. **31**(1): p. 37-42.
68. Soares, I.C., et al., *In silico analysis and immunohistochemical characterization of NaPi2b protein expression in ovarian carcinoma with monoclonal antibody Mx35*. Appl Immunohistochem Mol Morphol, 2012. **20**(2): p. 165-72.
69. Milenic, D.E., et al., *Targeting HER2: a report on the in vitro and in vivo pre-clinical data supporting trastuzumab as a radioimmunoconjugate for clinical trials*. MAbs, 2010. **2**(5): p. 550-64.
70. Heyerdahl, H., et al., *Targeted alpha therapy with 227Th-trastuzumab of intraperitoneal ovarian cancer in nude mice*. Curr Radiopharm, 2013. **6**(2): p. 106-16.
71. Weber, K.J. and M. Flentje, *Lethality of heavy ion-induced DNA double-strand breaks in mammalian cells*. Int J Radiat Biol, 1993. **64**(2): p. 169-78.

72. Kassis, A.I., *Therapeutic radionuclides: biophysical and radiobiologic principles*. Semin Nucl Med, 2008. **38**(5): p. 358-66.
73. Magnander, K. and K. Elmroth, *Biological consequences of formation and repair of complex DNA damage*. Cancer Lett, 2012. **327**(1-2): p. 90-6.
74. Sgouros, G., *Alpha-particles for targeted therapy*. Adv Drug Deliv Rev, 2008. **60**(12): p. 1402-6.
75. Humm, J.L., *Dosimetric aspects of radiolabeled antibodies for tumor therapy*. J Nucl Med, 1986. **27**(9): p. 1490-7.
76. Srinivasan, A. and S.K. Mukherji, *Tositumomab and iodine I 131 tositumomab (Bexaar)*. AJNR Am J Neuroradiol, 2011. **32**(4): p. 637-8.
77. Mondello, P., et al., *90 Y-ibritumomab tiuxetan: a nearly forgotten opportunity*. Oncotarget, 2015.
78. Wilbur, D.S., *Chemical and radiochemical considerations in radiolabeling with alpha-emitting radionuclides*. Curr Radiopharm, 2011. **4**(3): p. 214-47.
79. McDevitt, M.R., et al., *Radioimmunotherapy with alpha-emitting nuclides*. Eur J Nucl Med, 1998. **25**(9): p. 1341-51.
80. Apostolidis, C., et al., *Production of Ac-225 from Th-229 for targeted alpha therapy*. Analytical Chemistry, 2005. **77**(19): p. 6288-6291.
81. Larsen, R.H., B.W. Wieland, and M.R. Zalutsky, *Evaluation of an internal cyclotron target for the production of At-211 via the Bi-209 ($\alpha,2n$)At-211 reaction*. Applied Radiation and Isotopes, 1996. **47**(2): p. 135-143.
82. Zielinska, B., et al., *An improved method for the production of Ac-225/Bi-213 from Th-229 for targeted alpha therapy*. Solvent Extraction and Ion Exchange, 2007. **25**(3): p. 339-349.
83. Morgenstern, A., F. Bruchertseifer, and C. Apostolidis, *Bismuth-213 and actinium-225 -- generator performance and evolving therapeutic applications of two generator-derived alpha-emitting radioisotopes*. Curr Radiopharm, 2012. **5**(3): p. 221-7.
84. Spivakov, B.Y., et al., *Raman Laser Spectroscopic Studies of Bismuth(III) Halide-Complexes in Aqueous-Solutions*. Journal of Inorganic & Nuclear Chemistry, 1979. **41**(4): p. 453-455.
85. Zalutsky, M.R. and M. Pruszynski, *Astatine-211: production and availability*. Curr Radiopharm, 2011. **4**(3): p. 177-85.
86. Wilbur, D.S., *Radiohalogenation of proteins: an overview of radionuclides, labeling methods, and reagents for conjugate labeling*. Bioconjug Chem, 1992. **3**(6): p. 433-70.
87. Lindegren, S., T. Back, and H.J. Jensen, *Dry-distillation of astatine-211 from irradiated bismuth targets: a time-saving procedure with high recovery yields*. Appl Radiat Isot, 2001. **55**(2): p. 157-60.

88. Wilbur, D.S., et al., *Reagents for Astatination of Biomolecules. 6. An Intact Antibody Conjugated with a Maleimido-closo-Decaborate(2-) Reagent via Sulfhydryl Groups Had Considerably Higher Kidney Concentrations than the Same Antibody Conjugated with an Isothiocyanato-closo-Decaborate(2-) Reagent via Lysine Amines.* *Bioconjugate Chemistry*, 2012. **23**(3): p. 409-420.
89. Visser, G.W.M., E.L. Diemer, and F.M. Kaspersen, *The Nature of the Astatine-Protein Bond.* *International Journal of Applied Radiation and Isotopes*, 1981. **32**(12): p. 905-912.
90. Wilbur, D.S., et al., *Reagents for astatination of biomolecules: comparison of the in vivo distribution and stability of some radioiodinated/astatinated benzamidyl and nido-carboranyl compounds.* *Bioconjug Chem*, 2004. **15**(1): p. 203-23.
91. Wilbur, D.S., et al., *Reagents for astatination of biomolecules. 2. Conjugation of anionic boron cage pendant groups to a protein provides a method for direct labeling that is stable to in vivo deastatination.* *Bioconjugate Chemistry*, 2007. **18**(4): p. 1226-1240.
92. Wilbur, D.S., et al., *Reagents for Astatination of Biomolecules. 3. Comparison of closo-Decaborate(2-) and closo-Dodecaborate(2-) Moieties as Reactive Groups for Labeling with Astatine-211.* *Bioconjugate Chemistry*, 2009. **20**(3): p. 591-602.
93. Zalutsky, M.R. and A.S. Narula, *Astatination of Proteins Using an N-Succinimidyl Tri-Normal-Butylstannyl Benzoate Intermediate.* *Applied Radiation and Isotopes*, 1988. **39**(3): p. 227-232.
94. Garg, P.K., et al., *Synthesis of Radioiodinated N-Succinimidyl Iodobenzoate - Optimization for Use in Antibody Labeling.* *Applied Radiation and Isotopes*, 1989. **40**(6): p. 485-490.
95. Wilbur, D.S., et al., *Development of a Stable Radioiodinating Reagent to Label Monoclonal-Antibodies for Radiotherapy of Cancer.* *Journal of Nuclear Medicine*, 1989. **30**(2): p. 216-226.
96. Siegel, R.L., K.D. Miller, and A. Jemal, *Cancer Statistics, 2015.* *Ca-a Cancer Journal for Clinicians*, 2015. **65**(1): p. 5-29.
97. Andersson, H., et al., *Radioimmunotherapy of nude mice with intraperitoneally growing ovarian cancer xenograft utilizing At-211-labelled monoclonal antibody MOv18.* *Anticancer Research*, 2000. **20**(1A): p. 459-462.
98. Andersson, H., et al., *Comparison of the therapeutic efficacy of At-211- and I-131-labelled monoclonal antibody MOv18 in nude mice with intraperitoneal growth of human ovarian cancer.* *Anticancer Research*, 2001. **21**(1A): p. 409-412.
99. Elgqvist, J., et al., *Therapeutic efficacy and tumor dose estimations in radioimmunotherapy of intraperitoneally growing OVCAR-3 cells in nude mice with At-211-labeled monoclonal antibody MX35.* *Journal of Nuclear Medicine*, 2005. **46**(11): p. 1907-1915.

100. Elgqvist, J., *Fractionated radioimmunotherapy of intraperitoneally growing ovarian cancer in nude mice with 211At-MX35 (Fab')₂: therapeutic efficacy and myelotoxicity*. European Journal of Nuclear Medicine and Molecular Imaging, 2006. **33**: p. S115-S115.
101. Elgqvist, J., et al., *alpha-Radioimmunotherapy of intraperitoneally growing OVCAR-3 tumors of variable dimensions: Outcome related to measured tumor size and mean absorbed dose*. Journal of Nuclear Medicine, 2006. **47**(8): p. 1342-1350.
102. Elgqvist, J., *Administered activity and metastatic cure probability during radioimmunotherapy of ovarian cancer in nude mice with 211At-MX35 F(ab')₂*. European Journal of Nuclear Medicine and Molecular Imaging, 2006. **33**: p. S340-S340.
103. Palm, S., et al., *Therapeutic efficacy of astatine-211-labeled trastuzumab on radioresistant SKOV-3 tumors in nude mice*. International Journal of Radiation Oncology Biology Physics, 2007. **69**(2): p. 572-579.
104. Elgqvist, J., et al., *Repeated Intraperitoneal alpha-Radioimmunotherapy of Ovarian Cancer in Mice*. J Oncol, 2010. **2010**: p. 394913.
105. Andersson, H., et al., *Intraperitoneal alpha-Particle Radioimmunotherapy of Ovarian Cancer Patients: Pharmacokinetics and Dosimetry of (211)At-MX35 F(ab')₂(2)-A Phase I Study*. Journal of Nuclear Medicine, 2009. **50**(7): p. 1153-1160.
106. Cederkrantz, E., et al., *Absorbed Doses and Risk Estimates of (211)At-MX35 F(ab')₂ in Intraperitoneal Therapy of Ovarian Cancer Patients*. Int J Radiat Oncol Biol Phys, 2015. **93**(3): p. 569-76.
107. Cederkrantz, E., et al., *Absorbed Doses and Risk Estimates of At-211-MX35 F(ab')₂ in Intraperitoneal Therapy of Ovarian Cancer Patients*. International Journal of Radiation Oncology Biology Physics, 2015. **93**(3): p. 569-576.
108. Elgqvist, J., et al., *Administered activity and metastatic cure probability during radioimmunotherapy of ovarian cancer in nude mice with At-211-MX35 F(ab')₂*. International Journal of Radiation Oncology Biology Physics, 2006. **66**(4): p. 1228-1237.
109. Hamilton, T.C., et al., *Characterization of a Xenograft Model of Human Ovarian-Carcinoma Which Produces Ascites and Intraabdominal Carcinomatosis in Mice*. Cancer Research, 1984. **44**(11): p. 5286-5290.
110. Mattes, M.J., et al., *Mouse Monoclonal-Antibodies to Human Epithelial Differentiation Antigens Expressed on the Surface of Ovarian-Carcinoma Ascites-Cells*. Cancer Research, 1987. **47**(24): p. 6741-6750.

111. Mattes, M.J., K.O. Lloyd, and J.L. Lewis, Jr., *Binding parameters of monoclonal antibodies reacting with ovarian carcinoma ascites cells*. *Cancer Immunol Immunother*, 1989. **28**(3): p. 199-207.
112. Mitri, Z., T. Constantine, and R. O'Regan, *The HER2 Receptor in Breast Cancer: Pathophysiology, Clinical Use, and New Advances in Therapy*. *Chemother Res Pract*, 2012. **2012**: p. 743193.
113. Burstein, H.J., *The distinctive nature of HER2-positive breast cancers*. *N Engl J Med*, 2005. **353**(16): p. 1652-4.
114. Brollo, J., et al., *Adjuvant trastuzumab in elderly with HER-2 positive breast cancer: a systematic review of randomized controlled trials*. *Cancer Treat Rev*, 2013. **39**(1): p. 44-50.
115. Hudis, C.A., *Trastuzumab--mechanism of action and use in clinical practice*. *N Engl J Med*, 2007. **357**(1): p. 39-51.
116. Buza, N., D.M. Roque, and A.D. Santin, *HER2/neu in Endometrial Cancer: A Promising Therapeutic Target With Diagnostic Challenges*. *Arch Pathol Lab Med*, 2014. **138**(3): p. 343-50.
117. Santin, A.D., et al., *Trastuzumab treatment in patients with advanced or recurrent endometrial carcinoma overexpressing HER2/neu*. *Int J Gynaecol Obstet*, 2008. **102**(2): p. 128-31.
118. Aneheim, E., et al., *N-[2-(maleimido)ethyl]-3-(trimethylstannyl)benzamide, a molecule for radiohalogenation of proteins and peptides*. *Appl Radiat Isot*, 2015. **96**: p. 1-5.
119. Agarwal, P. and C.R. Bertozzi, *Site-specific antibody-drug conjugates: the nexus of bioorthogonal chemistry, protein engineering, and drug development*. *Bioconjug Chem*, 2015. **26**(2): p. 176-92.
120. Pippin, C.G., et al., *Spectrophotometric method for the determination of a bifunctional DTPA ligand in DTPA-monoclonal antibody conjugates*. *Bioconjug Chem*, 1992. **3**(4): p. 342-5.
121. Ingrand, J., *Characteristics of radio-isotopes for intra-articular therapy*. *Ann Rheum Dis*, 1973. **32 Suppl 6**: p. Suppl:3-9.
122. Elgqvist, J., et al., *Myelotoxicity and RBE of 211At-conjugated monoclonal antibodies compared with 99mTc-conjugated monoclonal antibodies and 60Co irradiation in nude mice*. *J Nucl Med*, 2005. **46**(3): p. 464-71.
123. Burbridge, M.F., et al., *Biological and pharmacological characterisation of three models of human ovarian carcinoma established in nude mice: use of the CA125 tumour marker to predict antitumour activity*. *Int J Oncol*, 1999. **15**(6): p. 1155-62.
124. Gahlen, J., et al., *Laparoscopic fluorescence diagnosis for intraabdominal fluorescence targeting of peritoneal carcinosis experimental studies*. *Ann Surg*, 2002. **235**(2): p. 252-60.
125. Peng, Q., et al., *5-Aminolevulinic acid-based photodynamic therapy. Clinical research and future challenges*. *Cancer*, 1997. **79**(12): p. 2282-308.

126. Tran Cao, H.S., et al., *Tumor-specific fluorescence antibody imaging enables accurate staging laparoscopy in an orthotopic model of pancreatic cancer*. *Hepatogastroenterology*, 2012. **59**(118): p. 1994-9.
127. Metildi, C.A., et al., *In vivo fluorescence imaging of gastrointestinal stromal tumors using fluorophore-conjugated anti-KIT antibody*. *Ann Surg Oncol*, 2013. **20 Suppl 3**: p. S693-700.
128. Liu, H. and K. May, *Disulfide bond structures of IgG molecules: structural variations, chemical modifications and possible impacts to stability and biological function*. *MAbs*, 2012. **4**(1): p. 17-23.
129. Yan, B.X., et al., *Human IgG1 Hinge Fragmentation as the Result of H2O2-mediated Radical Cleavage*. *Journal of Biological Chemistry*, 2009. **284**(51): p. 35390-35402.
130. Press, O.W., et al., *A comparative evaluation of conventional and pretargeted radioimmunotherapy of CD20-expressing lymphoma xenografts*. *Blood*, 2001. **98**(8): p. 2535-43.
131. Marshall, D., et al., *Polyethylene glycol modification of a galactosylated streptavidin clearing agent: effects on immunogenicity and clearance of a biotinylated anti-tumour antibody*. *Br J Cancer*, 1996. **73**(5): p. 565-72.
132. Caliceti, P., et al., *Poly(ethylene glycol)-avidin bioconjugates: suitable candidates for tumor pretargeting*. *J Control Release*, 2002. **83**(1): p. 97-108.
133. Meyer, D.L., et al., *Reduced antibody response to streptavidin through site-directed mutagenesis*. *Protein Sci*, 2001. **10**(3): p. 491-503.
134. Graves, S., et al., *Reduced antibody response to streptavidin through site directed mutagenesis*. *Faseb Journal*, 2000. **14**(6): p. A1135-A1135.
135. Hamblett, K.J., et al., *A streptavidin-biotin binding system that minimizes blocking by endogenous biotin*. *Bioconjug Chem*, 2002. **13**(3): p. 588-98.
136. Hamblett, K.J., et al., *Role of biotin-binding affinity in streptavidin-based pretargeted radioimmunotherapy of lymphoma*. *Bioconjug Chem*, 2005. **16**(1): p. 131-8.
137. Wilbur, D.S., et al., *Design and synthesis of bis-biotin-containing reagents for applications utilizing monoclonal antibody-based pretargeting systems with streptavidin mutants*. *Bioconjug Chem*, 2010. **21**(7): p. 1225-38.
138. Haraldsson, B., J. Nystrom, and W.M. Deen, *Properties of the glomerular barrier and mechanisms of proteinuria*. *Physiol Rev*, 2008. **88**(2): p. 451-87.
139. Pagel, J.M., et al., *Anti-CD45 pretargeted radioimmunotherapy using bismuth-213: high rates of complete remission and long-term*

- survival in a mouse myeloid leukemia xenograft model*. Blood, 2011. **118**(3): p. 703-11.
140. Frost, S., *Pretargeting agents and At-211-labeled effector molecules*, in *Radiation Physics 2012*, University of Gothenburg: Gothenburg.
141. Back, T. and L. Jacobsson, *The alpha-camera: a quantitative digital autoradiography technique using a charge-coupled device for ex vivo high-resolution bioimaging of alpha-particles*. J Nucl Med, 2010. **51**(10): p. 1616-23.
142. Sharkey, R.M. and D.M. Goldenberg, *Advances in radioimmunotherapy in the age of molecular engineering and pretargeting*. Cancer Invest, 2006. **24**(1): p. 82-97.
143. Dearling, J.L. and R.B. Pedley, *Technological advances in radioimmunotherapy*. Clin Oncol (R Coll Radiol), 2007. **19**(6): p. 457-69.